Nkx2-5+/Islet1+ mesenchymal precursors generate distinct spleen stromal cell subsets and participate in restoring stromal network integrity

Laura Castagnaro[1], Elisa Lenti[1], Laura Spinardi[2], Sara Maruzzelli[1], Edoardo Migliori[1], Diego Farinello[1], Giovanni Sitia[3], Zachary Harrelson[4], Sylvia Evans[4], Luca G. Guidotti[3,5], Richard P. Harvey[6] and Andrea Brendolan[1*]

[1]Division of Molecular Oncology and [3]Division of Immunology, Transplantation and Infectious Diseases, San Raffaele Scientific Institute, Milan, 20132 Italy; [2]Fondazione IRCCS Ca' Granda Ospedale Maggiore Policlinico, Milan, 20122 Italy, [4]Skaggs School of Pharmacy and Pharmaceutical Sciences and Department of Medicine, University of California, San Diego, CA, 92093 USA; [5]Department of Immunology & Microbial Sciences, The Scripps Research Institute, La Jolla, CA, 92037 USA; [6]The Victor Chang Cardiac Research Institute, Darlinghurst, New South Wales, 2010, and St. Vincent's Clinical School, University of New South Wales, Kensington 2052, Australia.

Running title: Nkx2-5/Islet1+ progenitors for spleen stromal cells

[*]**Address correspondence to:**

Andrea Brendolan

Laboratory of Lymphoid Organ Development

Division Molecular Oncology, DIBIT-1, 3A2

San Raffaele Scientific Institute

Via Olgettina 60, 20132 Milan, Italy

Phone 39+ 02-26434719

Fax 39+ 02-26434844

Email brendolan.andrea@hsr.it

Abstract

Lymphoid organ stromal cells comprise different subsets whose origin remains unknown. **Herein, we exploit a genetic lineage-tracing approach to show that, with the exception of endothelial cells, fibroblastic reticular cells (FRCs), follicular dendritic cells (FDCs), marginal reticular cells (MRCs) and mural cells of the spleen originate from embryonic mesenchymal progenitors of the Nkx2-5+/Islet1+ lineage. This lineage includes embryonic mesenchymal cells** with lymphoid tissue organizer (LTo) activity capable of supporting ectopic lymphoid-like structures, and **a subset of resident spleen stromal cells that proliferate and regenerate the splenic stromal microenvironment following resolution of a viral infection. These findings reveal a lineage-restricted mechanism involved in generating stromal diversity and in lymphoid tissue repair and remodeling.**

I. Introduction.

While much is known about the immunological function of the spleen, knowledge of the mechanisms governing the development and organization of its stromal microenvironment is still rudimentary. During mouse development, specification of splenic mesenchymal cells occurs at embryonic (E) day 10-10.5 within the dorsal spleno-pancreatic mesenchyme (SPM) and relies on the expression of a limited set of homedomain transcription factor-encoding genes (Brendolan et al., 2007; Dear et al., 1995; Hecksher-Sorensen et al., 2004). Among these, *Nkx2-5* marks newly specified splenic progenitors in the SPM and in the splenic primordium thereafter (Brendolan et al., 2005; Burn et al., 2008); and its requirement for spleen development has been recently demonstrated (Koss et al., 2012). The homeodomain protein Islet1 is also expressed in the dorsal pancreatic mesenchyme, and its loss of function allele in mice causes agenesis of the dorsal pancreatic mesenchyme (Ahlgren et al., 1997). However, its role in spleen development has not been elucidated since Islet1 mutants die in utero prior to initiation of spleen development (Ahlgren et al., 1997). Of note, ablation of the dorsal pancreatic mesenchyme at E10.5 with diphtheria toxin was recently shown to cause agenesis of both the pancreas and spleen in mice (Landsman et al., 2011), thus demonstrating the requirement for mesenchymal cells of the SPM in spleen organogenesis.

Once specified, splenic mesenchymal cells expand within the dorsal mesogastrium to form the splenic anlage (Brendolan et al., 2007). **At mid-gestation, spleen mesenchymal cells include** lymphoid tissue organizer (LTo) cells that are thought to be precursors for adult stromal cells of secondary lymphoid organs[not clear if you mean secondary to spleen or secondary to BM including spleen; are you suggesting that spleen cells migrate to eg nodes?] (Katakai et al., 2008; Koning and Mebius, 2011; Mueller and Germain, 2009; Vondenhoff et al., 2008). Whether splenic LTo cells are capable of organizing the formation of lymphoid compartments and generating the

different stromal cell subsets remains unknown. Mature stromal cells have been described based on their topological location and the expression of homeostatic chemokines such as CCL19, CCL21 and CXCL13 and they include gp38+ fibroblastic reticular cells (FRCs) (Link et al., 2007; Onder et al., 2011) of the T-cell area, CD35+ follicular dendritic cells (FDCs) (Allen and Cyster, 2008; Cyster et al., 2000) of the B-cell area, MAdCAM1+ marginal reticular cells (MRCs) (Katakai et al., 2008; Mebius and Kraal, 2005) of the marginal zone, endothelial and perivascular cells (Lax et al., 2007; Mueller and Germain, 2009). At present, the paucity of markers for lineage-tracing analysis has limited our understanding of the origin and lineage restriction of both LTo and adult stromal cells. FRCs and MRCs have been proposed to derive from LTo cells (Benezech et al., 2010; Koning and Mebius, 2011), although their embryonic precursors have not been identified yet. FRCs can also arise in the adult spleen subsequent to pathological conditions, as illustrated by experiments in which mice were infected with the lymphocytic choriomeningitis virus (LCMV) (Mueller et al., 2007; Scandella et al., 2008). These experiments indicate that FRC-infected cells, once destroyed by the LCMV-specific adaptive immune response, are replaced by stromal cells of unknown origin (Mueller et al., 2007; Scandella et al., 2008). CXCL13-expressing FDCs are the major stromal cell type of the B-cell follicle for which a mesenchymal origin has been proposed (Cyster et al., 2000; Krautler et al., 2012; Mabbott et al., 2011; Munoz-Fernandez et al., 2006). Similar to FRCs and MRCs, it remains unclear whether FDCs derive from embryonic mesenchymal progenitors or whether they migrate to the SLO postnatally (Allen and Cyster, 2008; Mabbott et al., 2011; Munoz-Fernandez et al., 2006). Endothelial and mural cells (smooth muscle cells and pericytes) (Lax et al., 2007; Onder et al., 2011) of the spleen are also part of the stromal network, however, similar to the other stromal cell subsets their origin and lineage restriction are currently unknown.

Herein we performed lineage-tracing analysis to assess the developmental relationships

between newly specified spleen mesenchymal progenitors of the dorsal spleno-pancreatic mesenchyme and the adult stromal cell pool. We show that with the exception of PECAM-1+ endothelial cells, all spleen stromal cells originate from embryonic mesenchymal precursors of the Nkx2-5+/Islet1+ lineage. Furthermore, we demonstrate that mesenchymal cells **included** in this lineage organize the lymphoid microenvironment and participate in regeneration of the adult FRC-stromal network after resolution of an acute LCMV infection. These findings reveal a previously unknown mechanism for generating distinct subsets of spleen stromal cells.

Results

Co-expression of Nkx2-5 and Islet1 is confined to the newly specified spleen mesenchymal progenitors

Given that both Nkx2.5 and Islet1 are expressed at E10-10.5 in the dorsal pancreatic mesenchyme (Ahlgren et al., 1997; Hecksher-Sorensen et al., 2004), and that *Nkx2.5* marks the newly specified progenitors of the SPM (Brendolan et al., 2005; Burn et al., 2008), we sought to test whether Islet1 is also expressed in spleen mesenchymal progenitors. Immunofluorescence analyses performed on transverse E10.5 mouse sections revealed co-localization of Nkx2-5 and Islet1 proteins in mesenchymal cells of the SPM (Fig 1A). Co-expression of Nkx2-5 and Islet1 was restricted to mesenchymal cells positioned on the left-lateral side of the dorsal pancreas (Fig. 1A inset) where spleen progenitors are known to localize (Burn et al., 2008; Hecksher-Sorensen et al., 2004). By E13.5 Islet1 was no longer detectable yet Nkx2-5 remained expressed in mesenchymal cells of the splenic primordium (Fig. 1B). These findings indicate that co-expression of Nkx2-5 and Islet1 is restricted to newly specified spleen mesenchymal progenitors of the SPM.

The Nkx2-5+/Islet1+ lineage generates FRCs, MRCs and FDCs

Co-localization of Nkx2-5 and Islet1 in the SPM raises the possibility that these transcription factors mark an early mesenchymal progenitor for adult spleen stromal cells, as they do for heart progenitors (Cai et al., 2003; Laugwitz et al., 2008; Moretti et al., 2006). To follow the fate of Nkx2-5+ and Islet1+ mesenchymal descendents, we crossed knock-in *Nkx2-5*$^{Cre/+}$ or *Islet1*$^{Cre/+}$ mice (Stanley et al., 2002; Yang et al., 2006), in which Cre expression is directed to the dorsal pancreatic mesenchyme, to *RosaYFP* reporter mice (Srinivas et al., 2001) that express yellow fluorescence protein (YFP) upon Cre-mediated recombination. Under these conditions, YFP expression in Nkx2-5+ or Islet1+ descendents remains permanent and independent of continuous Cre expression.

In adult spleen, Nkx2-5 YFP+ descendents showed a reticular pattern consistent with a contribution to stromal cells but not to CD45+ lymphoid cells **(Suppl. Fig. 1A-B)**, whereas Islet1 contributed both to stromal and to some CD45+ lymphoid cells **(Suppl. Fig. 2A-B)**. Consistent with the loss of Islet1 protein at early stages (E13.5) of spleen development (Fig. 1) immunofluorescence analysis performed on adult spleen **revealed expression of Islet1 in some CD45+ cells and rare CD45- cells that are not stromal cells (Suppl. Fig. 2C, arrows).**

To better characterize Islet1 stromal contribution and minimize the presence of Islet1 lymphoid descendents in the spleen, we performed Cre recombinase-based fate mapping in lethally irradiated *Islet1*$^{Cre/+}$*;RosaYFP* adult compound mice reconstituted with wild type bone marrow cells (Bajenoff et al., 2008). Detection of YFP in the adult spleen of those mice would reveal selective contribution of the Islet1+ lineage to radio-resistant stromal cells. Animals were allowed to recover for 8 weeks to ensure complete reconstitution of hematopoietic-derived cells (Bajenoff et al., 2008). Notably, the density and distribution of **YFP+** stromal cells in the spleen of those mice were found comparable to those of **non-irradiated, non-transplanted controls, thus excluding that irradiation altered the pattern distribution of the stromal cell pool.** Immunofluorescence analysis of adult spleens from *Nkx2-5*$^{Cre/+}$*;RosaYFP* mice or *Islet1*$^{Cre/+}$*;RosaYFP* chimeric mice revealed the presence of YFP+ reticular cells in the white pulp. Assessment of gp38/Podoplanin and ERTR-7 expression and **quantification of desmin+ cells co-expressing YFP** showed that the large majority of FRCs were YFP+ thus indicating a contribution of Nkx2-5+ or the Islet1+ lineages to T-cell zone stromal cells **(Fig. 2A and Suppl. Fig. 3A).** FRCs also form the splenic conduit system, a network of collagenous channels ensheathed by fibroblasts (Nolte et al., 2003). To visualize the conduit and determine the fibroblastic nature of YFP+ cells in this area, adult *Nkx2-5*$^{+/Cre}$*;RosaYFP* mice were injected with fluorescently labeled dextran (Bajenoff et al., 2006; Nolte et al., 2003; Sixt

et al., 2005). The analysis revealed that YFP+ cells juxtaposed the collagenous channels, thus contributing to form the conduit system **(Suppl. Fig. 4)**. The presence of YFP+ cells in the marginal zone (MZ) of adult *Nkx2-5$^{Cre/+}$;RosaYFP* mice and *Islet1$^{Cre/+}$;RosaYFP* chimeric mice prompted us to analyze the expression of markers for marginal reticular cells (MRCs) (i.e. MAdCAM-1 and CXCL13) (Katakai et al., 2008). The distribution of YFP+ cells co-expressing MAdCAM-1 and CXCL13 and **quantification of CXCL13+ cells expressing YFP** in the marginal zone revealed that, like FRCs, virtually all MRCs originate from the Nkx2-5+/Islet1+ lineage **(Fig. 2B and Suppl. Fig. 3B).** As CXCL13+YFP+ cells were additionally observed in areas corresponding to the B-cell follicles, we assessed whether these cells corresponded to FDCs. Staining YFP+ cells with the FDC specific markers CD35 and CXCL13, and **quantification of CXCL13+ FDCs expressing YFP** revealed a large degree of co-localization **(Fig. 2C and Suppl. Fig. 3C)**, suggesting that FDCs arise from mesenchymal progenitors belonging to the Nkx2-5+/Islet1+ lineage.

To exclude the possibility that YFP+ FRCs, MRCs and FDCs derive from Nkx2-5+ or Islet1+ mesenchymal cells which have migrated to the spleen postnatally, embryonic spleens (E16.5) from *Nkx2-5$^{Cre/+}$;RosaYFP* and *Islet1$^{Cre/+}$;RosaYFP* fetuses were transplanted under the kidney capsule of adult wild type mice that were subsequently immunized with sheep red blood cells to promote FDC-network formation (Glanville et al., 2009; Schnizlein et al., 1985). Under these conditions, T- and B-cell compartments displaying features similar to those of the adult spleen are known to develop in about 4 weeks of transplantation (Glanville et al., 2009). The finding that virtually all gp38+ FRCs, CXCL13+ MRCs, and CD35+ FDCs in transplanted spleens were also YFP+ indicates that these stromal cells derive from embryonic Nkx2-5+/Islet1+ mesenchymal precursors **(Fig. 3).**

The Nkx2-5+/Islet1+ lineage generates mural, but not endothelial cells

The presence of YFP signal surrounding the central arteriole in the T-cell area (Fig. 2A) prompted us to determine whether Nkx2-5+ and Islet1+ lineages could generate endothelial cells (expressing PECAM-1) and/or mural cells (expressing αSMA and the neuronal/glial 2 proteoglycan [NG2] (Feng et al., 2011)). Immunofluorescence analysis revealed that PECAM-1 did not co-localize with YFP+ cells **(Fig. 4),** indicating no contribution of the Nkx2-5+ and Islet1+ lineages to endothelial cells of the spleen white pulp. Conversely, YFP+ cells surrounding the central arteriole expressed αSMA and NG2 **(Fig. 4)**, thus indicating a contribution of Nkx2-5+ and Islet1+ lineages to smooth muscle cells and pericytes.

Embryonic Nkx2-5+/Islet1+ descendents include cells with lymphoid tissue organizer activity

The finding that Nkx2-5+/Islet1+ lineage gives rise to all stromal cell subsets coupled with the notion that LTo cells may represent the precursors of mature stromal cells (Katakai et al., 2008; Koning and Mebius, 2011; Vondenhoff et al., 2008), suggests that the embryonic Nkx2-5+/Islet1+ lineage **includes cells with organizer capacity**. To test this hypothesis, we first purified CD45-YFP+ and CD45-YFP- mesenchymal cells from E18.5 *Nkx2-5$^{Cre/+}$;RosaYFP* spleens and performed qPCR analysis to assess the expression of markers previously used to define the LTo cells (Vondenhoff et al., 2008) (e.g. the receptor for lymphotoxin β [LTβR], the vascular cell adhesion protein-1 [VCAM-1], and the chemokine CXCL13). The analyses revealed that CD45-YFP+ mesenchymal cells express mRNA levels for *LTβR, ICAM-1, VCAM-1, CCL19*, *CXCL13,* and ***IL-7*** that are significantly higher than those detected in CD45-YFP- cells simultaneously purified which, in contrast, expressed endothelial cell markers (e.g. *PECAM-1* and *CCL21*) more abundantly (Vondenhoff et al., 2008) **(Fig. 5A)**. **To determine whether E18.5 YFP+ progenitors include cells that can be classified as LTo also based on their capacity to support lymphocyte survival via**

IL-7, we cultured sorted (E18.5) primary YFP+ cells of the Nkx2-5+/Islet1+ lineage together with naïve CD4 T cells. The results indicated that spleen mesenchymal cells support the survival of naïve CD4 T cells very efficiently, though this effect was not mediated exclusively by IL-7 (Suppl. Fig. 5), and showed that under these conditions, the embryonic splenic mesenchyme secrete other factors that compensate IL-7 depletion in promoting lymphocyte survival.

We next exploited a model of artificial lymphoid organ formation (Suematsu and Watanabe, 2004) by using Nkx2-5+ embryonic mesenchymal cells as a source of stromal progenitors. Sorted E18.5 CD45-YFP+ cells were embedded into a biocompatible collagenous scaffold that was subsequently transplanted under the kidney capsule of wild type mice (Fig. 5B). Three weeks after transplantation scaffolds were harvested and analysis of their composition revealed juxtaposed T- and B-cell clusters resembling normal lymphoid architecture (Fig. 5C). In addition, we found that the relative number of CD4+ and CD8+ T-cell subsets were similar (data not shown) and lymphoid clusters were vascularized, as demonstrated by expression of the endothelial marker PECAM-1 (Fig. 5C). CD45-YFP+ mesenchymal cells were distributed either inside or immediately outside lymphoid clusters to form a stromal network (Fig. 5C). Notably, similar experiments with sorted CD45-YFP- cells, as a source of stromal progenitors, produced scaffolds containing only few and scattered T cells (Suppl. Fig. 6), indicating that cells with stromal organizer capacity were **included** only in the Nkx2-5+/Islet1+ lineage.

A subset of the Nkx2-5+/Islet1+ descendents restores the stromal network integrity after resolution of LCMV infection

As descendents of the Nkx2-5+ lineage display organizer activity, we assessed their capacity to organize and restore the stromal integrity after resolution of an acute LCMV infection (Iannacone

et al., 2008). Using this model, others have shown that LCMV-infected FRCs are killed by LCMV-specific CD8+ T cells within 8 days of infection, resulting in the collapse of the splenic stromal network (Mueller et al., 2007; Scandella et al., 2008). The network is restored in about four weeks after infection (e.g. approximately two weeks after viral clearance has occurred), although the nature of the stromal cells involved in this process remains unknown. First, adult *Nkx2-5$^{Cre/+}$;RosaYFP* mice were infected with LCMV and their spleens analyzed 4 days after infection, a time at which viremia is maximal (Iannacone et al., 2008; Mueller et al., 2007) (Suppl. Fig. 7A). At this stage, YFP+ cells staining positive for the LCMV nucleoprotein (visualized by VL4 antibody) were observed in T- and B-cell areas and in the marginal zone (Suppl. Fig. 7B arrowheads). Conversely, YFP+ perivascular cells, including NG2+ pericytes surrounding the central arteriole, stained negative for the LCMV nucleoprotein (Suppl. Fig. 7B arrows), indicating that the virus does not target these cells.

At day 8 after LCMV infection, the YFP+ FRC stromal network, adjacent to the B-cell follicle (Fig. 6), was highly disorganized as indicated by reduced expression of the FRC-associated extracellular matrix component laminin (Sixt et al., 2005) and by the number of YFP+ stromal cells that were much reduced when compared to uninfected controls (Fig. 6). At this stage, **the lymphoid compartment was also disorganized as revealed by loss of T-cell areas (Suppl. Fig. 8A).** The same analysis performed 40 days after infection revealed that the expression of laminin and the distribution of YFP+ in the FRC area surrounding the central arteriole was comparable to that of uninfected control mice at day 8 **and this was accompanied by restoration of the T-cell zones (Fig. 6 and Suppl. Fig. 8)**, thus indicating that **a subset of** YFP+ cells of the Nkx2-5+/Islet1+ lineage contribute to rebuild the integrity of the stromal network after resolution of LCMV infection. **To assess whether stromal regeneration occurred via expansion of resident YFP+ descendents,**

LCMV-infected *Nkx2-5$^{Cre/+}$;RosaYFP* mice were administered with a bolus of the BrdU analog EdU (5-ethynyl-2´-deoxyuridine) on day 20 post infection and their spleen analyzed 16 hrs later for the presence of proliferating cells. At this stage, restoration of the stromal network has already started to occur (Scandella REF), and immunofluorescence analysis revealed a significant increase of YFP+ EdU+ proliferating cells in LCMV-infected mice as compared to uninfected controls (Fig. 7A). To establish if these YFP+ cells were derived from resident cells or from Nkx2-5-expressing cells that have migrated into the spleen from the periphery, we transplanted E16.5 wild type spleens under the kidney capsule of *Nkx2-5$^{Cre/+}$;RosaYFP* reporter mice. Five weeks after transplantation, mice were infected with LCMV and transplanted spleens analyzed for the presence of YFP+ cells four weeks after. To confirm that transplanted spleens had been infected, we analyzed spleen architecture 10 days after LCMV and found largely disorganized lymphoid compartments (not shown), indicating that the virus indeed reached the transplant. Analysis performed on transplanted spleens on day 28, a time when the stromal network has been largely restored (Scandella et al., 2008), revealed organized lymphoid compartments and absence of YFP+ stromal networks in these wild type heterotypic explants into *Nkx2-5$^{Cre/+}$;RosaYFP* mice (Fig. 7B), further indicating that restoration of stromal integrity was mediated by a fraction of resident proliferating Nkx2-5+/Islet1+ descendents and not by cells that migrate into the organ.

Discussion

We show here that adult spleen stromal cells are developmentally related to newly specified spleen mesenchymal cells of the SMP that, in addition to Nkx2-5, express the homeodomain transcription factor Islet1, a previously unknown marker for spleen mesenchymal cells. While Nkx2-5 expression in mesenchymal cells is maintained throughout development, Islet1 expression is transiently regulated and lost in mesenchymal cells of the newly formed splenic anlage. A similar temporal relationship is seen for Islet1 and Nkx2-5 in heart development (Cai et al., 2003; Laugwitz et al., 2008; Sun et al., 2007). Taking advantage of Islet1 transient expression in Nkx2.5+ spleen progenitor cells, we performed recombinase-based fate mapping under the control of two independent Cre driver mouse lines to identify the contribution of Nkx2-5+/Islet1+ mesenchymal descendents of the SPM to the adult stromal cell pool. **Our immunofluorescence and quantification analyses** showed that both Nkx2-5+ and Islet1+ lineages generate all spleen stromal cell subsets, namely FRCs, MRCs, FDCs and mural cells, **indicating** that they represent a common mesenchymal lineage for adult stromal cells. These lineage-tracing experiments, however, while suggesting an embryonic origin for the different stromal cell subsets, they do not exclude the possibility that cells expressing Cre in other locations (e.g. blood) and migrating into the spleen postnatally, contribute to specific stromal cell subsets. To address these questions, we transplanted embryonic (E16.5) *Nkx2-5$^{Cre/+}$;RosaYFP* or *Islet1$^{Cre/+}$;RosaYFP* spleens into wild type recipients and found that gp38+ (FRCs), CXCL13+ (MRCs), CD35+ (FDCs) cells co-expressed YFP, indicating they originate from resident embryonic Nkx2-5+/Islet1+ descendents. Although these transplantation experiments cannot exclude the possibility that Nkx2-5+/Islet1+ cells migrate to the embryonic spleen from other organs (e.g. fetal liver) prior to transplantation (E16.5), the transient expression of Islet1 in Nkx2-5+ spleen mesenchymal cells of the SMP at E10.5, **the wide distribution of Nkx2-5+ mesenchymal cells in the splenic anlage prior to transplantation,**

together with the findings that Nkx2-5 does not contribute to hematopoietic cells argue against this hypothesis, and strongly support the conclusion that Nkx2.5+/Islet1+ mesenchymal descendents of the nascent splenic anlage are the main source of mature stromal cells. The conclusion that FDCs originate from mesenchymal precursors is further supported by recent findings showing that PDGFRβ+ perivascular cells of stromal origin are the source of FDCs (Krautler et al., 2012). Although a dual-fluorescence reporter allele will be required to unequivocally demonstrate that spleen stromal cells arise from a double-positive progenitor, the finding that co-expression of Nkx2-5 and Islet1 is restricted to newly specified spleen mesenchymal progenitors of the SPM together with the recent demonstration that Islet1 and Nkx2-5 are also co-expressed in multipotent mesodermal progenitors that contributes to several cardiac lineages at a clonal level indicate the existence of multipotent mesenchymal precursors for adult spleen stromal cells (Laugwitz et al., 2008; Moretti et al., 2006).

Previous studies showed that the differentiating splenic mesenchyme consists of LTo and endothelial cells that have been characterized based on the expression of phenotypic markers (Vondenhoff et al., 2008). The finding that E18.5-sorted CD45-YFP+ mesenchymal cells of the Nkx2-5+/Islet1+ lineage display higher levels of LTo cell markers (e.g. *LTβR, VCAM-1, CXCL13* ***and IL-7***) as compared to CD45-YFP- cells that, conversely, express endothelial cell markers (e.g. PECAM-1), suggests that the Nkx2.5+/Islet1+ lineage also **includes** LTo cells. **Although sorted E18.5 YFP+ mesenchymal cells efficiently supported the survival of naïve lymphocytes, the effect was not exclusively mediated by IL-7. These findings indicate that, although embryonic spleen mesenchymal cells of the Nkx2-5+/Islet1+ lineage express IL-7, other factors compensate for IL-7 depletion in promoting lymphocyte survival. The finding that that FRCs, MRCs, FDCs and mural cells derive from the Nkx2-5+/Islet1+ mesenchymal lineage when**

***Nkx2-5$^{Cre/+}$;RosaYFP* or *Islet1$^{Cre/+}$;RosaYFP* embryonic spleens were transplanted under the kidney capsule of wild type mice further support the hypothesis that LTo cells are the embryonic precursors of adult stromal cells (Koning and Mebius, 2011)**. By definition, LTo cells should be capable of organizing the formation of lymphoid compartments, and we addressed this by exploiting a model of artificial lymphoid organ formation (Suematsu and Watanabe, 2004). We found that only E18.5 sorted mesenchymal cells (LTo) of the Nkx2-5+/Islet1+ lineage promote the development of ectopic lymphoid microenvironments characterized by T- and B-cell clusters and YFP+ stromal cell networks, thus confirming that the Nkx2-5+/Islet1+ lineage possesses organizer activity. However, contrary to whole embryonic spleen transplants, YFP+ stromal cells present in the ectopic lymphoid clusters did not express FRC, MRC and FDC markers. This indicates that under these conditions, YFP+ cells are limited in their organizer capacity to promote T and B cell clusters and suggest that signals needed for their maturation are lost when cells are disaggregated, sorted and embedded into the biocompatible scaffold. Nevertheless, the LTo-like gene expression profile of the sorted CD45-YFP+ cells, their *ex vivo* capacity to support the formation of lymphoid compartments, together with their *in vivo* potential (E16.5 transplanted spleens) to generate FRCs, MRCs, FDCs and mural cells, strongly indicates that the Nkx2-5+/Islet1+ lineage **includes a fraction of cells classified as stromal organizer cells.**

Since no adult stromal lineage had been formerly documented to function as organizer of stromal compartments, we also sought to test whether the Nkx2-5+/Islet1+ descendents are capable of regenerating the stromal integrity after LCMV infection. Notably, remodeling and organization of the stromal network after resolution of an acute LCMV infection have been recently shown to depend, at least in part, on the presence of LTi cells (Eberl et al., 2004; Scandella et al., 2008; Withers et al., 2007), however the origin of the mesenchymal cells that contribute to re-establish

stromal network integrity has not been investigated. Consistent with being a lineage **that includes LTo cells, we found that Nkx2-5/Islet1 descendents participate in rebuilding the FRC stromal network after LCMV infection. Our transplantation experiments also indicate that regeneration of the stromal network depends on the expansion of resident Nkx2-5+/Islet1+ descendents, possibly possessing mesenchymal stem cell-like activity, and does not involved migration of Nkx2-5+ stromal precursors from the periphery**. Altogether these findings strongly support the conclusion that stromal cells that are **included** in the Nkx2-5+/Islet1+ lineage function as organizer cells during tissue remodeling. **This scenario is in line with recent findings that described a population of heart-resident mesenchymal stem-like cells with a developmental origin and long-term persistence *in vivo* (Chong et al., 2011). Although the nature of the cells that participate in the regeneration of the spleen stromal network is still unclear, we observed that splenic YFP+ perivascular cells (e.g. pericytes), recently suggested to function as mesenchymal stem cells (Crisan et al., 2008; Dellavalle et al., 2011; Feng et al., 2011), are not targeted by LCMV, thus raising the interesting possibility that this cell type serves as a reservoir of local stromal progenitors during tissue regeneration. Notably, the recent finding that mature FDCs arise from PDGFRβ+ perivascular cells, and that ablation of the latter population causes loss of FDC+ networks and profound disorganization of the T-cell stromal network strongly indicate a role for perivascular cells in tissue development and remodeling (Krautler et al., 2012).**

These studies demonstrate that the embryonic splenic mesenchyme is the source of virtually all stromal cell subsets. Based on these findings, we propose a model for spleen stromagenesis in which the expression of *Nkx2-5* and *Islet1* marks newly specified spleen mesenchymal progenitors that differentiate into intermediate cellular elements **capable to generate** FDCs, FRCs, MRCs, and perivascular cells. Our results begin to define the cellular mechanisms responsible for generating the

stromal diversity and those implicated in lymphoid tissue remodeling.

ACKNOWLEDGEMENTS

The authors are grateful to R. Aiolfi for technical assistance. A. Mondino and K. Pilipow for helpful suggestions and reagents. We thank Jorge Caamano, Reina Mebius, Serge van der Pavert, Giovanni Tonon and Federico Caligaris-Cappio for critically reading the manuscript. This work was supported by: Associazione Italiana Ricerca sul Cancro (AIRC) (Start-Up Grant #4780 to A.B. and Special Program Molecular Clinical Oncology - 5 per mille #9965); Marie Curie Foundation (IRG-2007 #208932 to A.B); Italian Ministry of Health (GR08.17 to G.S); National Institute of Health, USA (R01-AI40696 to L.G.G), National Health and Medical Research Council, Australia (573705, 573703 to R.P.H). SME acknowledges funding from NIH.

AUTHOR CONTRIBUTIONS

L.C., S.M., E.L., L.S., G.S., L.G.G. and A.B. performed the experiments and analyzed data, S.E., L.G.G and R.P.H provided mouse lines and reagents, A.B. wrote the manuscript with the contribution of L.G.G., and R.P.H., and A.B. directed the study.

COMPETING FINANCIAL INTERESTS

The authors declare no competing financial interests.

MATERIAL AND METHODS

Mice

Nkx2-5$^{Cre/+}$, *Islet1*$^{Cre/+}$, *R26R-EYFP* (Srinivas et al., 2001; Stanley et al., 2002; Yang et al., 2006) mice have been previously described. Mice were breed and maintained at San Raffaele Scientific Institute and The Scripps Research Institute in pathogen-free rooms under barrier conditions, and all experiments were performed according to local ethics committee regulations. For the generation of chimeras, *Islet1*$^{Cre/+}$*;RosaYFP* mice were irradiated with two 4,5Gy cycles from a cesium source and reconstituted with 1x10^7 C57BL/6 total bone marrow cells. Detection of vaginal plug was designated as E0.5.

Immunofluorescece stainings

Spleens and kidney containing scaffolds were harvested and fixed for 5' PFA 4% (Sigma), washed in phosphate buffer saline, and dehydrated over night 30% in sucrose (Sigma). Embryos were fixed in 20' PFA 4% (Sigma), washed in phosphate buffer saline, and dehydrated over night 30% in sucrose (Sigma). Samples were embedded in Tissue-Tek OCT compound (Bio-optica) and frozen in ethanol dry ice bath. 7mm thick sections were placed onto glass slides (Bio-optica), fixed in cold acetone for 10 minutes, dried and kept at -80°C until used. Slides were incubated 30 min with a blocking solution of PBS-Tween 0.05% plus 0,5% FBS. Primary antibodies and secondary antibodies and streptavidin reagents (Supplementary table 1) were diluted in blocking solution and incubated for one hour and thirties minutes respectively. For mouse antibodies, MOM blocking solution (Vector Lab) was used. Nuclei were visualized with DAPI (Fluka), and mounting performed with Moviol (Calbiochem). For detection of MAdCAM-1, CXCL13, and gp38 antibodies Tyramide Signal Amplification kit (Perkin Elmer) was used. To visualized conduit system, 10kDa Dextran Alexa-546 conjugated (Molecular Probe) was injected i.v. Images were acquired using

Ultraview Zeiss or Leica TCS SP2 laser confocal microscopes. Digital images were recorded in separately scanned channels with no overlap in detection of emissions from the respective fluorochromes. Final image processing was performed with Adobe Illustrator and Photoshop.

Cell sorting, isolation of primary cells and transplantation

E18.5 spleens from *Nkx2-5$^{+/Cre}$;RosaYFP* embryos were isolated and digested using a buffer containing 0.45mg/ml of Liberase TL (Roche) and 0.5mg/ml DnaseI (Roche) in phosphate buffered saline (PBS) containing 2% Fetal Calf Serum (FBS). Digestion was performed under constant agitation (140 rpm) for 30 minutes at 37°C and disaggregation obtained by pipetting to obtain a single-cell suspension. Cells were washed twice in PBS 2% FBS, suspended in PBS with 5% FBS and filtered with on a 70 mm mesh. CD45-YFP+ and CD45-YFP- cells isolated using a fluorescence activated cell sorter Vantage (BD) and suspended in PBS prior to transplantation.

Protocol for generation of artificial lymphoid-like structures was previously described(Suematsu and Watanabe, 2004). In brief, cell suspension was placed onto collagenous matrix (CS-35; Koken) and squeezed several times to allow cell adsorption into the scaffold. Scaffolds containing cells were kept on ice and transplanted under one kidney capsule of anesthetized C57BL/6 mice as previously described (Suematsu and Watanabe, 2004). Three weeks later scaffolds were collected, fixed and analyzed by immunofluorescence staining. Transplantation of embryonic spleens under the kidney capsule was performed as previously described (Glanville et al., 2009). In brief, E16.5 spleens from *Nkx2-5$^{+/Cre}$;RosaYFP* were isolated and immediately transplanted under the renal subcapsular space of C57BL/6 mice as described above. Three weeks after transplantation, mice were immunized by i.v. injection of $2x10^8$ sheep red blood cells as previously described (Schnizlein et al., 1985), and one week later spleens were collected, fixed and analyzed by immunofluorescence microscopy analysis.

Lymphocyte survival assay

Single cell suspension from sorted E18.5 YFP+ cells were plated in 24-wells plate at a density of 200.000 cells/well and cultured in complete RPMI 1640 medium (containing 10% FBS). After 48 hour expansion, non-adherent cells were removed, cells were harvested and re-plated at a concentration of 250.000 cells/well in a 24-wells plate with the addition of magnetically purified CD4+ lymphocytes from adult LNs at a ratio of 4:1. After four days of co-culture with anti-IL-7Ra blocking and isotype control antibody (Biolegend), non adherent lymphocytes were harvested, the number of live cells was determined by Trypan blue dye exclusion, and cells were stained with CD4 and the viability dye To-Pro3 (Invitrogen). The percentage of surviving cells after four days of culture was obtained after normalizing the total number of viable naive CD62^{high} CD4^{+} cells with that of lymphocytes alone cultured with recombinant IL-7 (Peprotech).

RNA isolation and quantitative RT-PCR

RNA was extracted from sorted cells using the RNeasy Micro kit (Qiagen). Reverse transcription of total RNA was performed with the ImProm-II Reverse Transcrption System kit with random primers (Promega). qPCR were performed using Universal Probe Library system (Roche) on a LightCycler480 (Roche). The C_t of the *Rpl13* (housekeeping) was subtracted from the C_t of the target gene and the relative expression was calculated as $2^{-\Delta C}{}_t$. qPCR were performed in triplicate and mean ± SD represented as relative expression. Primer sequences are described in supplementary table 2. qPCR experiments were done using cDNA from three different cell sorting experiments.

LCMV infections and in vivo proliferation

Eight week-old *Nkx2-5$^{+/Cre}$;RosaYFP* mice were injected i.v. with 200 plaque-forming unit of

lymphocytic chroriomeningitis virus (LCMV) clone WE or with phosphate saline buffer. Serum LCMV RNA was analyzed by qPCR as described (McCausland and Crotty, 2008) using the following LCMV-specific primers: 5-CTCCTTTCCCAAGAGAAGACTAAG-3 and 5-TCCATTTGGTCAGGCAATAAC-3. At days 4, 8 or 40 after LCMV infection, mice were sacrificed and their spleen were collected, fixed 5 min in 4% PFA (Sigma), washed in phosphate buffer saline, and dehydrated over night 30% in sucrose (Sigma) prior of embedding. **To assess proliferation, 1 mg/mouse of 5-ethynyl-2´-deoxyuridine (EdU) was injected intraperitoneum in PBS and evaluated 16 hrs later according to manufacture instructions (Invitrogen). Proliferation was measured by counting the number of EdU+ YFP+ cells over the total EdU+ cells from 12 high magnification fields of 3 mice analyzed for each condition.**

Statistical analysis

Statistical analysis was performed with Prism (GraphPad Software 5a) and values are expressed as mean ± SD. Means between two groups were compared by using a two-tailed t-test. Differences were considered statistically significant at $p < 0.05$.

FIGURE LEGENDS

Figure 1. Co-expression of Nkx2-5 and Islet1 in spleen mesenchymal progenitors

Fluorescence confocal images of dorsal pancreatic mesenchyme at E10.5 (**A**), and splenic anlage at E13.5 (**B**). Expression of Islet1 (red) and Nkx2-5 (green) (**A**) in newly specified spleen mesenchymal cells positioned on the left-lateral side of the dorsal pancreas at E10.5 (inset in **A**), and in splenic primordium at E13.5 thereafter (**B**). Higher magnification areas are from mid-panel insets in **A** and **B** respectively**.** Nuclei are visualized by DAPI staining (blue). Scale bars, 100 μm for low and 35 μm for high magnifications. SPM, spleno pancreatic mesenchyme; DP, dorsal pancreas; SP, spleen primordium; ST stomach. Data are representative of three embryos analyzed.

Figure 2. The Nkx2-5+/Islet1+ lineages generate FRCs, MRCs and FDCs

Representative confocal images of *Nkx2-5$^{Cre/+}$;Rosa26YFP* and *Islet1$^{Cre/+}$;Rosa26YFP* adult spleen sections stained for YFP as a marker of Nkx2-5 and Islet1 lineage-traced cells (green in **A**, **B**, **C**) and gp38/Podoplanin and ERTR7 (red in **A)**; MAdCAM-1 and CXCL13 (red in **B)**; CD35 and CXCL13 (red in **C)** to show the contribution of Nkx2-5+ and Islet1+ lineages to FRCs, MRCs and FDCs respectively. Higher magnification areas are from insets in **A**, **B**, **and C.** Nuclei are visualized by DAPI staining (blue). Scale bars, 100 μm for low and 35 μm for high magnifications. WP, white pulp; CA, central arteriole. Data are representative of four to five mice analyzed.

Figure 3. FRCs, MRCs, and FDCs arise from embryonic Nkx2-5+/Islet1+ descendents

Representative confocal images of *Nkx2-5$^{Cre/+}$;Rosa26YFP* and *Islet1$^{Cre/+}$;Rosa26YFP* embryonic (E16.5) spleens transplanted under the kidney capsule of wild type mice and stained for YFP (green in **A**, **B**, **C**), gp38 (red in **A**), CXCL13 (red in **B**) and CD35 (red in **C**) to show contribution of

embryonic lineage-traced cells to FRCs, MRCs, and FDCs (arrows indicate merge). Higher magnification areas are from insets. Nuclei are visualized by DAPI staining (blue). Scale bars, 100 μm for low and 35 μm for high magnifications. WP, white pulp; MZ, marginal zone. Data are representative of four mice analyzed.

Figure 4. Nkx2-5+/Islet1+ lineages give rise to mural cells

Representative confocal images of *Nkx2-5$^{Cre/+}$;Rosa26YFP* (**A**) and *Islet1$^{Cre/+}$;Rosa26YFP* (**B**) adult spleen sections stained for YFP (green in **A-B)**, PECAM-1 (red in **A, B,** left panel), αSMA (red in **A, B** mid-panel), and NG2 (red in **A, B** right panel) to show the contribution of Nkx2-5+ and Islet1+ lineage-traced cells to endothelial (arrowheads) and mural cells (arrows). Higher magnification areas are from insets. Nuclei are visualized by DAPI staining (blue). Scale bars, 100 μm for low and 35 μm for high magnifications. WP: white pulp, CA: central arteriole. Data are representative of three mice analyzed.

Figure 5. Lymphoid tissue organizer cells are included in Nkx2-5+/Islet1+ descendents

Expression of LTo associated markers by sorted embryonic (E18.5) CD45-YFP+ and CD45-YFP- mesenchymal cells **(A)**. Values are presented as the ratio of the gene of interest to *Rpl13* housekeeping gene and expressed as relative expression. Differences were considered statistically significant at $p < 0.05$. Scheme for generating artificial lymphoid-like structures (**B**). Sorted CD45-YFP+ and CD45-YFP- cells from embryonic (E18.5) *Nkx2-5$^{Cre/+}$;Rosa26YFP* spleens were embedded in a collagenous scaffold and transplanted under the kidney capsule of wild type mice. Representative confocal images of scaffolds harvested three weeks after transplantation (**C**) and stained for CD3, B220, PECAM-1, and YFP. Lymphoid clusters are indicated with dashed circles. Nuclei are visualized by DAPI staining (blue). Scale bars indicate 100μm. Data are representative of

four transplanted mice.

Figure 6. A subset of Nkx2-5+/Islet1+ descendents regenerates the stromal network after resolution of viral infection

Representative confocal images of spleen sections from *Nkx2-5$^{Cre/+}$;Rosa26YFP* mice injected with PBS (Ctrl) or with 200 plaque forming unit of LCMV WE (LCMV) and stained for YFP (green) as a marker for lineage-traced cells, laminin (red) to visualized the FRC-associated ECM network, and B220 (blue) to detect B-cell follicles. Arrows indicate YFP+ perivascular cells surrounding central arteriole. Higher magnification areas are from insets. Scale bars, 100 μm for low and 35 μm for high magnifications. MZ, marginal zone; CA, central arteriole. Data are representative of four experiments with two mice each group.

Figure 7. Restoration of stromal network integrity occurs via expansion of resident Nkx2-5+/Islet1+ descendents

Representative confocal images of spleen sections from *Nkx2-5$^{Cre/+}$;Rosa26YFP* mice after LCMV infection and stained for EdU (green) to visualize proliferating cells and YFP (red) to detect Nkx2-5/Islet1 stromal descendents. (**A**). Arrows indicate YFP+ proliferating stromal cells. Percentage of proliferating YFP+ cells in LCMV infected and control mice (**B**). Assessment of 12 high power fields per spleen from 3 mice analyzed for each group. Scheme of embryonic spleen transplantation (**C**). Representative confocal images of transplanted spleen sections stained for CD3 (red) and YFP (green). Nuclei are visualized by DAPI staining (blue). Scale bar, 75 μm magnification. MZ, marginal zone; CA, central arteriole. Data are representative of three mice analyzed for each group.

SUPPLEMENTARY FIGURE LEGENDS

Suppl. Figure 1. Contribution of Nkx2-5+ lineage-traced cells to the adult spleen

Representative confocal images of adult *Nkx2-5$^{Cre/+}$;Rosa26YFP* spleen sections stained for YFP (green) to visualized lineage-traced cells and CD45+ (red) to reveal lymphoid cells (**A**). Confocal images of adult spleen sections stained for B220, CD3, F4/80 ,Ter119 and YFP (**B**). Nuclei are visualized by DAPI staining (blue). Higher magnification are from insets. Scale bars, 100 μm for low and 35 μm for high magnifications. CA, central arteriole; WP, white pulp; RP, red pulp; B, B-cell area; T, T-cell area. Data are representative of three mice analyzed.

Suppl. Figure 2. Contribution of Islet1+ lineage-traced cells to the adult spleen

Representative confocal images of adult *Islet1$^{Cre/+}$;Rosa26YFP* spleen sections stained for YFP (green) to visualized lineage-traced cells and CD45+ (red) to reveal lymphoid cells (**A**). Confocal images of adult spleen sections stained for B220, CD3, F4/80, Ter119 and YFP (**B**). Expression of Islet1 (red), CD45 and stromal cells (green in left and right panels respectively) in adult spleen (**C**). Nuclei are visualized by DAPI staining (blue). Higher magnifications are from insets. Scale bars, 100 μm for low and 50 μm for high magnifications. CA, central arteriole; WP, white pulp; RP, red pulp; B, B-cell area; T, T-cell area. Data are representative of three mice analyzed.

Suppl. Figure 3. Quantification of FRCs, FDCs, and MRCs relative to lineage-traced cells

Representative confocal images of adult *Nkx2-5$^{Cre/+}$;Rosa26YFP* and *Islet1$^{Cre/+}$;Rosa26YFP* spleen sections stained for YFP (**A, B, C**), desmin (**A**), and CXCL13 (**B** and **C**). Scale bar, 100 μm. Values indicate the percentage of FRCs (desmin+), MRCs (CXCL13+) and FDCs (CXCL13+) derived-signals overlapping with YFP signal from lineage-traced stromal cells. For each lineage,

assessment of 8 high-power fields were analyzed.

Suppl. Figure 4. Nkx2-5+ lineage contributes to form the T-cell area conduit system

Representative confocal image of adult spleen sections from *Nkx2-5$^{Cre/+}$;Rosa26YFP* mice injected with 10 kDa dextran Alexa 546 conjugated (red) and stained for YFP to visualized lineage-traced cells (green). Arrowheads indicate YFP+ cells associated with dextran+ conduit channels. Scale bars, 35 μm. Data are representative of three mice analyzed.

Suppl. Figure 5. Lineage-traced embryonic mesenchyme support lymphocyte survival independently of IL-7.

Percentages of CD62^{high} CD4^{+} T cell survival cultured alone (white bars), in the presence of recombinant IL-7 (black bars) or co-cultured with E18.5 mesenchymal cells of the Nkx2-5+/Islet1+ lineage in the presence (light dray) or absence (dark dray) of an anti-IL-7Rα blocking antibody for four days. Mean of quadruplicates ± SD are represented, and data are from one of two independent experiments.

Suppl. Figure 6. CD45- YFP- stromal cells do not possess LTo activity

Representative confocal images of collagenous scaffolds embedded with sorted CD45-YFP- cells from embryonic (E18.5) *Nkx2-5$^{Cre/+}$;Rosa26YFP* spleens and transplanted under the kidney capsule of wild type mice. Scaffolds harvested three weeks after transplantation and stained for CD3 (red) and B220 (green) show the presence of only scattered T-cells. Higher magnification area is from inset. Scale bars, 100 μm. Data are representative of four transplanted mice.

Suppl. Figure 7. LCMV viremia and distribution of LCMV infected cells

Nkx2-5$^{Cre/+}$;Rosa26YFP mice were injected i.v. with 200 plaque forming unit of LCMV WE and mean (± standard deviation) of genome equivalents (GE) at the indicated time points are indicated (**A**). Ctrl, saline injected controls. Data are representative of four experiments with two mice each group.

Representative confocal images of spleen sections from *Nkx2-5$^{Cre/+}$;Rosa26YFP* mice 4 days after LCMV WE infection stained for YFP (lineage-traced cells, green), NG2 (perivascular cells, red), CD35 (FDCs, red), MAdCAM1(MRCs, red) and LCMV nucleoprotein (VL4 antibody, blue) (**B**). Arrowheads indicate colocalization of LCMV nucleoprotein and YFP in stromal cells of the T-area, B-area and marginal zone. Arrows indicate not infected YFP+ cells. Higher magnifications are from insets. Scale bars, 100 μm for low and 35 μm for high magnifications. CA, central arteriole; MZ, marginal zone. Data are representative of three mice analyzed.

Suppl. Figure 8. Organization of lymphoid compartments during resolution of LCMV infection

Representative confocal images of spleen sections from *Nkx2-5$^{Cre/+}$;Rosa26YFP* mice (**A, B)** injected with PBS (Ctrl) or with 200 plaque forming unit of LCMV WE (**A, B),** and stained for B220 and CD3 (**A**) or F4/80 and CD11b (**B**) to visualized the lymphoid compartments 8 and 40 days post infection. Scale bars, 100 μm magnifications. Ctrl, control; CA, central arteriole; MZ, marginal zone. Data are representative of four experiments with two mice each group.

REFERENCES

Ahlgren, U., Pfaff, S.L., Jessell, T.M., Edlund, T., and Edlund, H. (1997). Independent requirement for ISL1 in formation of pancreatic mesenchyme and islet cells. Nature *385*, 257-260.

Allen, C.D., and Cyster, J.G. (2008). Follicular dendritic cell networks of primary follicles and germinal centers: phenotype and function. Semin Immunol *20*, 14-25.

Bajenoff, M., Egen, J.G., Koo, L.Y., Laugier, J.P., Brau, F., Glaichenhaus, N., and Germain, R.N. (2006). Stromal cell networks regulate lymphocyte entry, migration, and territoriality in lymph nodes. Immunity *25*, 989-1001.

Bajenoff, M., Glaichenhaus, N., and Germain, R.N. (2008). Fibroblastic reticular cells guide T lymphocyte entry into and migration within the splenic T cell zone. J Immunol *181*, 3947-3954.

Benezech, C., White, A., Mader, E., Serre, K., Parnell, S., Pfeffer, K., Ware, C.F., Anderson, G., and Caamano, J.H. (2010). Ontogeny of stromal organizer cells during lymph node development. J Immunol *184*, 4521-4530.

Brendolan, A., Ferretti, E., Salsi, V., Moses, K., Quaggin, S., Blasi, F., Cleary, M.L., and Selleri, L. (2005). A Pbx1-dependent genetic and transcriptional network regulates spleen ontogeny. Development *132*, 3113-3126.

Brendolan, A., Rosado, M.M., Carsetti, R., Selleri, L., and Dear, T.N. (2007). Development and function of the mammalian spleen. Bioessays *29*, 166-177.

Burn, S.F., Boot, M.J., de Angelis, C., Doohan, R., Arques, C.G., Torres, M., and Hill, R.E. (2008). The dynamics of spleen morphogenesis. Dev Biol *318*, 303-311.

Cai, C.L., Liang, X., Shi, Y., Chu, P.H., Pfaff, S.L., Chen, J., and Evans, S. (2003). Isl1 identifies a cardiac progenitor population that proliferates prior to differentiation and contributes a majority of cells to the heart. Dev Cell *5*, 877-889.

Chong, J.J., Chandrakanthan, V., Xaymardan, M., Asli, N.S., Li, J., Ahmed, I., Heffernan, C.,

Menon, M.K., Scarlett, C.J., Rashidianfar, A., *et al.* (2011). Adult cardiac-resident MSC-like stem cells with a proepicardial origin. Cell Stem Cell *9*, 527-540.

Crisan, M., Yap, S., Casteilla, L., Chen, C.W., Corselli, M., Park, T.S., Andriolo, G., Sun, B., Zheng, B., Zhang, L., *et al.* (2008). A perivascular origin for mesenchymal stem cells in multiple human organs. Cell Stem Cell *3*, 301-313.

Cyster, J.G., Ansel, K.M., Reif, K., Ekland, E.H., Hyman, P.L., Tang, H.L., Luther, S.A., and Ngo, V.N. (2000). Follicular stromal cells and lymphocyte homing to follicles. Immunol Rev *176*, 181-193.

Dear, T.N., Colledge, W.H., Carlton, M.B., Lavenir, I., Larson, T., Smith, A.J., Warren, A.J., Evans, M.J., Sofroniew, M.V., and Rabbitts, T.H. (1995). The Hox11 gene is essential for cell survival during spleen development. Development *121*, 2909-2915.

Dellavalle, A., Maroli, G., Covarello, D., Azzoni, E., Innocenzi, A., Perani, L., Antonini, S., Sambasivan, R., Brunelli, S., Tajbakhsh, S., and Cossu, G. (2011). Pericytes resident in postnatal skeletal muscle differentiate into muscle fibres and generate satellite cells. Nat Commun *2*, 499.

Eberl, G., Marmon, S., Sunshine, M.J., Rennert, P.D., Choi, Y., and Littman, D.R. (2004). An essential function for the nuclear receptor RORgamma(t) in the generation of fetal lymphoid tissue inducer cells. Nat Immunol *5*, 64-73.

Feng, J., Mantesso, A., De Bari, C., Nishiyama, A., and Sharpe, P.T. (2011). Dual origin of mesenchymal stem cells contributing to organ growth and repair. Proc Natl Acad Sci U S A *108*, 6503-6508.

Glanville, S.H., Bekiaris, V., Jenkinson, E.J., Lane, P.J., Anderson, G., and Withers, D.R. (2009). Transplantation of embryonic spleen tissue reveals a role for adult non-lymphoid cells in initiating lymphoid tissue organization. Eur J Immunol *39*, 280-289.

Hecksher-Sorensen, J., Watson, R.P., Lettice, L.A., Serup, P., Eley, L., De Angelis, C., Ahlgren, U.,

and Hill, R.E. (2004). The splanchnic mesodermal plate directs spleen and pancreatic laterality, and is regulated by Bapx1/Nkx3.2. Development *131*, 4665-4675.

Iannacone, M., Sitia, G., Isogawa, M., Whitmire, J.K., Marchese, P., Chisari, F.V., Ruggeri, Z.M., and Guidotti, L.G. (2008). Platelets prevent IFN-alpha/beta-induced lethal hemorrhage promoting CTL-dependent clearance of lymphocytic choriomeningitis virus. Proc Natl Acad Sci U S A *105*, 629-634.

Katakai, T., Suto, H., Sugai, M., Gonda, H., Togawa, A., Suematsu, S., Ebisuno, Y., Katagiri, K., Kinashi, T., and Shimizu, A. (2008). Organizer-like reticular stromal cell layer common to adult secondary lymphoid organs. J Immunol *181*, 6189-6200.

Koning, J.J., and Mebius, R.E. (2011). Interdependence of stromal and immune cells for lymph node function. Trends Immunol *33*, 264-270.

Koss, M., Bolze, A., Brendolan, A., Saggese, M., Capellini, T.D., Bojilova, E., Boisson, B., Prall, O.W., Elliott, D.A., Solloway, M., *et al.* (2012). Congenital Asplenia in Mice and Humans with Mutations in a Pbx/Nkx2-5/p15 Module. Dev Cell *22*, 913-926.

Krautler, N.J., Kana, V., Kranich, J., Tian, Y., Perera, D., Lemm, D., Schwarz, P., Armulik, A., Browning, J.L., Tallquist, M., *et al.* (2012). Follicular dendritic cells emerge from ubiquitous perivascular precursors. Cell *150*, 194-206.

Landsman, L., Nijagal, A., Whitchurch, T.J., Vanderlaan, R.L., Zimmer, W.E., Mackenzie, T.C., and Hebrok, M. (2011). Pancreatic mesenchyme regulates epithelial organogenesis throughout development. PLoS Biol *9*, e1001143.

Laugwitz, K.L., Moretti, A., Caron, L., Nakano, A., and Chien, K.R. (2008). Islet1 cardiovascular progenitors: a single source for heart lineages? Development *135*, 193-205.

Lax, S., Hou, T.Z., Jenkinson, E., Salmon, M., MacFadyen, J.R., Isacke, C.M., Anderson, G., Cunningham, A.F., and Buckley, C.D. (2007). CD248/Endosialin is dynamically expressed on a

subset of stromal cells during lymphoid tissue development, splenic remodeling and repair. FEBS Lett *581*, 3550-3556.

Link, A., Vogt, T.K., Favre, S., Britschgi, M.R., Acha-Orbea, H., Hinz, B., Cyster, J.G., and Luther, S.A. (2007). Fibroblastic reticular cells in lymph nodes regulate the homeostasis of naive T cells. Nat Immunol *8*, 1255-1265.

Mabbott, N.A., Kenneth Baillie, J., Kobayashi, A., Donaldson, D.S., Ohmori, H., Yoon, S.O., Freedman, A.S., Freeman, T.C., and Summers, K.M. (2011). Expression of mesenchyme-specific gene signatures by follicular dendritic cells: insights from the meta-analysis of microarray data from multiple mouse cell populations. Immunology *133*, 482-498.

McCausland, M.M., and Crotty, S. (2008). Quantitative PCR technique for detecting lymphocytic choriomeningitis virus in vivo. J Virol Methods *147*, 167-176.

Mebius, R.E., and Kraal, G. (2005). Structure and function of the spleen. Nat Rev Immunol *5*, 606-616.

Moretti, A., Caron, L., Nakano, A., Lam, J.T., Bernshausen, A., Chen, Y., Qyang, Y., Bu, L., Sasaki, M., Martin-Puig, S., *et al.* (2006). Multipotent embryonic isl1+ progenitor cells lead to cardiac, smooth muscle, and endothelial cell diversification. Cell *127*, 1151-1165.

Mueller, S.N., and Germain, R.N. (2009). Stromal cell contributions to the homeostasis and functionality of the immune system. Nat Rev Immunol *9*, 618-629.

Mueller, S.N., Matloubian, M., Clemens, D.M., Sharpe, A.H., Freeman, G.J., Gangappa, S., Larsen, C.P., and Ahmed, R. (2007). Viral targeting of fibroblastic reticular cells contributes to immunosuppression and persistence during chronic infection. Proc Natl Acad Sci U S A *104*, 15430-15435.

Munoz-Fernandez, R., Blanco, F.J., Frecha, C., Martin, F., Kimatrai, M., Abadia-Molina, A.C., Garcia-Pacheco, J.M., and Olivares, E.G. (2006). Follicular dendritic cells are related to bone

marrow stromal cell progenitors and to myofibroblasts. J Immunol *177*, 280-289.

Nolte, M.A., Belien, J.A., Schadee-Eestermans, I., Jansen, W., Unger, W.W., van Rooijen, N., Kraal, G., and Mebius, R.E. (2003). A conduit system distributes chemokines and small blood-borne molecules through the splenic white pulp. J Exp Med *198*, 505-512.

Onder, L., Scandella, E., Chai, Q., Firner, S., Mayer, C.T., Sparwasser, T., Thiel, V., Rulicke, T., and Ludewig, B. (2011). A Novel Bacterial Artificial Chromosome-Transgenic Podoplanin-Cre Mouse Targets Lymphoid Organ Stromal Cells in vivo. Front Immunol *2*, 50.

Scandella, E., Bolinger, B., Lattmann, E., Miller, S., Favre, S., Littman, D.R., Finke, D., Luther, S.A., Junt, T., and Ludewig, B. (2008). Restoration of lymphoid organ integrity through the interaction of lymphoid tissue-inducer cells with stroma of the T cell zone. Nat Immunol *9*, 667-675.

Schnizlein, C.T., Kosco, M.H., Szakal, A.K., and Tew, J.G. (1985). Follicular dendritic cells in suspension: identification, enrichment, and initial characterization indicating immune complex trapping and lack of adherence and phagocytic activity. J Immunol *134*, 1360-1368.

Sixt, M., Kanazawa, N., Selg, M., Samson, T., Roos, G., Reinhardt, D.P., Pabst, R., Lutz, M.B., and Sorokin, L. (2005). The conduit system transports soluble antigens from the afferent lymph to resident dendritic cells in the T cell area of the lymph node. Immunity *22*, 19-29.

Srinivas, S., Watanabe, T., Lin, C.S., William, C.M., Tanabe, Y., Jessell, T.M., and Costantini, F. (2001). Cre reporter strains produced by targeted insertion of EYFP and ECFP into the ROSA26 locus. BMC Dev Biol *1*, 4.

Stanley, E.G., Biben, C., Elefanty, A., Barnett, L., Koentgen, F., Robb, L., and Harvey, R.P. (2002). Efficient Cre-mediated deletion in cardiac progenitor cells conferred by a 3'UTR-ires-Cre allele of the homeobox gene Nkx2-5. Int J Dev Biol *46*, 431-439.

Suematsu, S., and Watanabe, T. (2004). Generation of a synthetic lymphoid tissue-like organoid in mice. Nat Biotechnol *22*, 1539-1545.

Sun, Y., Liang, X., Najafi, N., Cass, M., Lin, L., Cai, C.L., Chen, J., and Evans, S.M. (2007). Islet 1 is expressed in distinct cardiovascular lineages, including pacemaker and coronary vascular cells. Dev Biol *304*, 286-296.

Vondenhoff, M.F., Desanti, G.E., Cupedo, T., Bertrand, J.Y., Cumano, A., Kraal, G., Mebius, R.E., and Golub, R. (2008). Separation of splenic red and white pulp occurs before birth in a LTalphabeta-independent manner. J Leukoc Biol *84*, 152-161.

Withers, D.R., Kim, M.Y., Bekiaris, V., Rossi, S.W., Jenkinson, W.E., Gaspal, F., McConnell, F., Caamano, J.H., Anderson, G., and Lane, P.J. (2007). The role of lymphoid tissue inducer cells in splenic white pulp development. Eur J Immunol *37*, 3240-3245.

Yang, L., Cai, C.L., Lin, L., Qyang, Y., Chung, C., Monteiro, R.M., Mummery, C.L., Fishman, G.I., Cogen, A., and Evans, S. (2006). Isl1Cre reveals a common Bmp pathway in heart and limb development. Development *133*, 1575-1585.

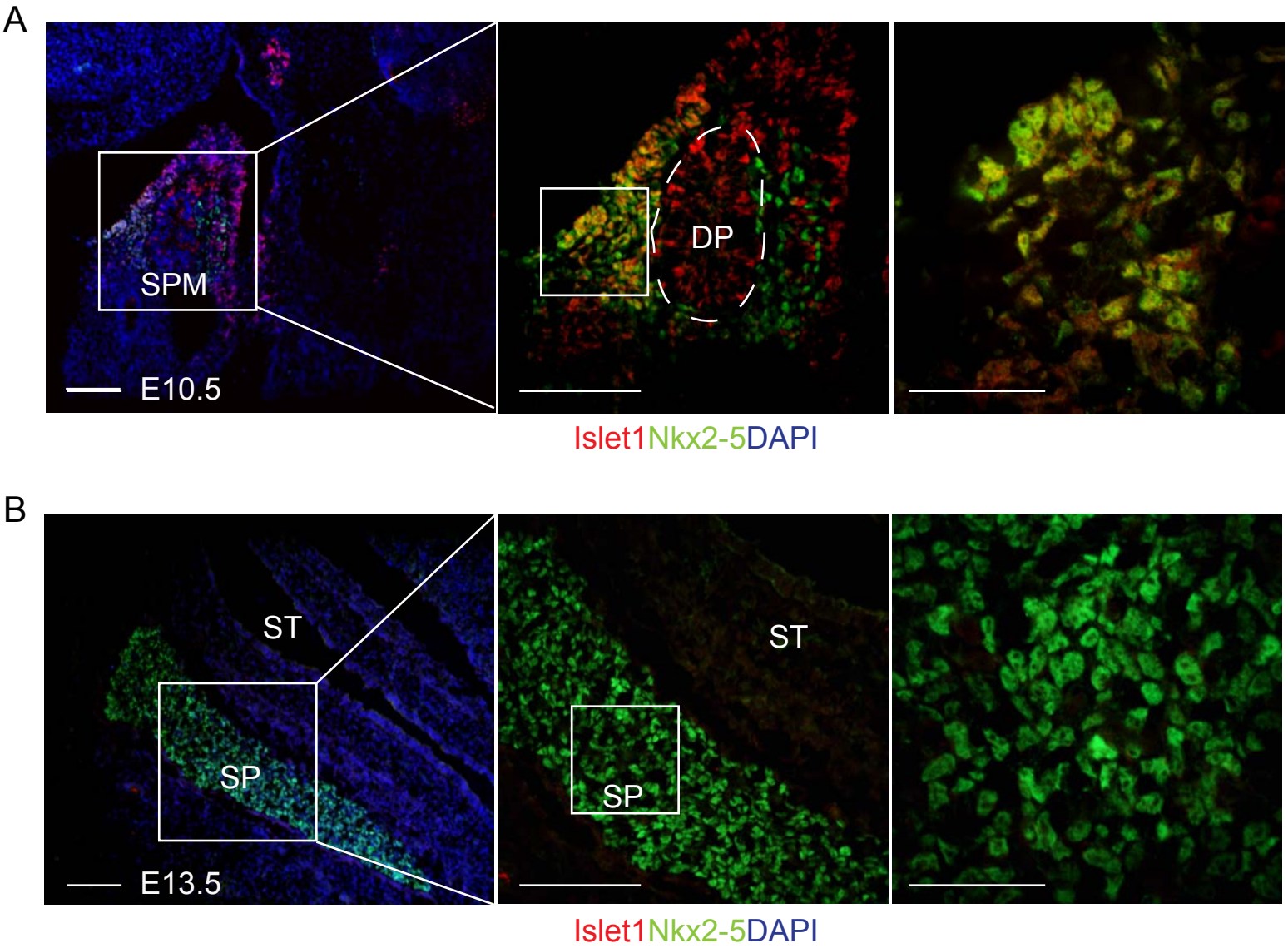
A
SPM
E10.5
DP
Islet1Nkx2-5DAPI
B
ST
SP
E13.5
ST
SP
Islet1Nkx2-5DAPI

Figure 1

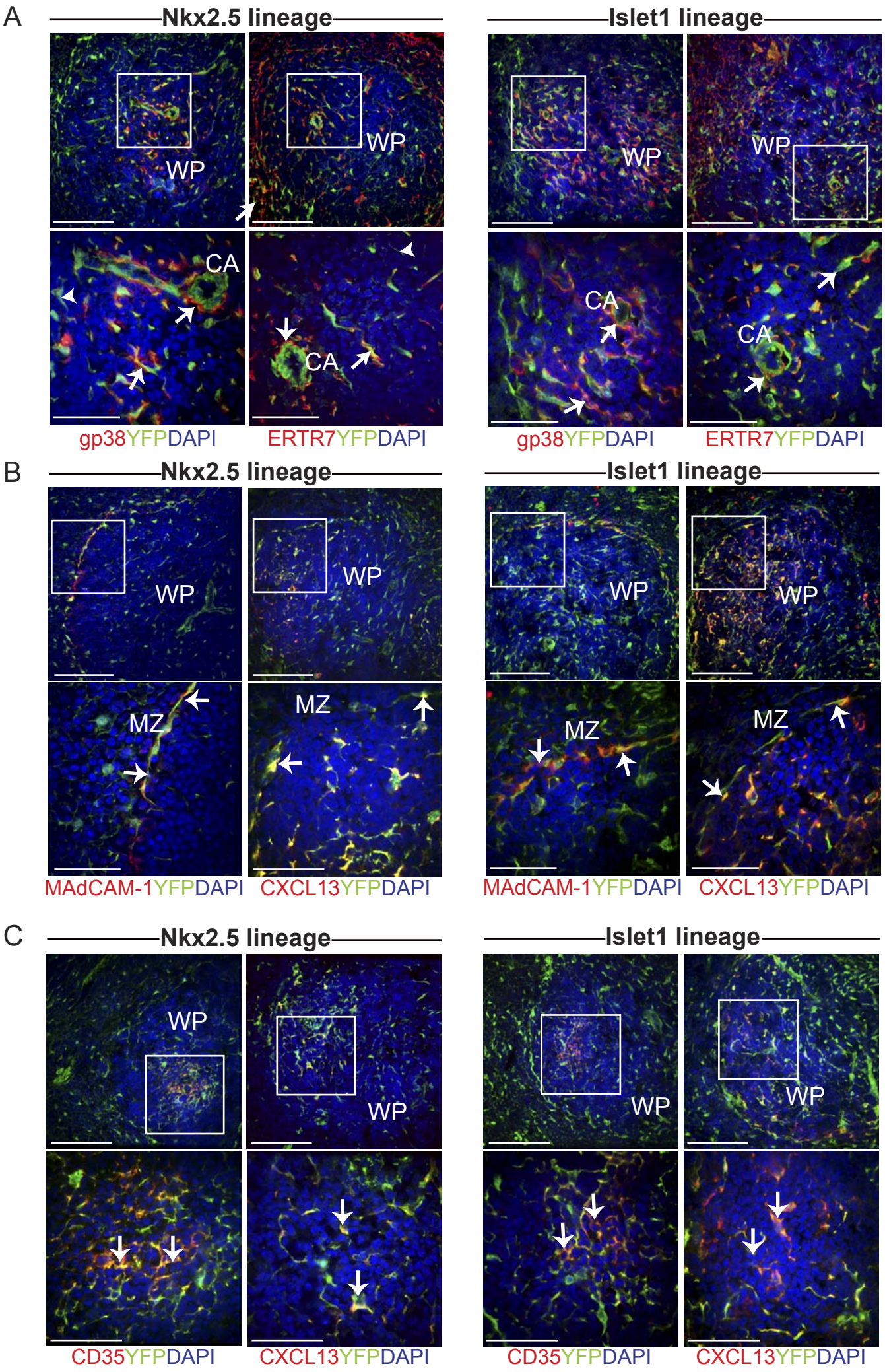
A
Nkx2.5 lineage
Islet1 lineage
WP
CA
gp38YFPDAPI
ERTR7YFPDAPI
B
MZ
MAdCAM-1YFPDAPI
CXCL13YFPDAPI
C
CD35YFPDAPI

Figure 2

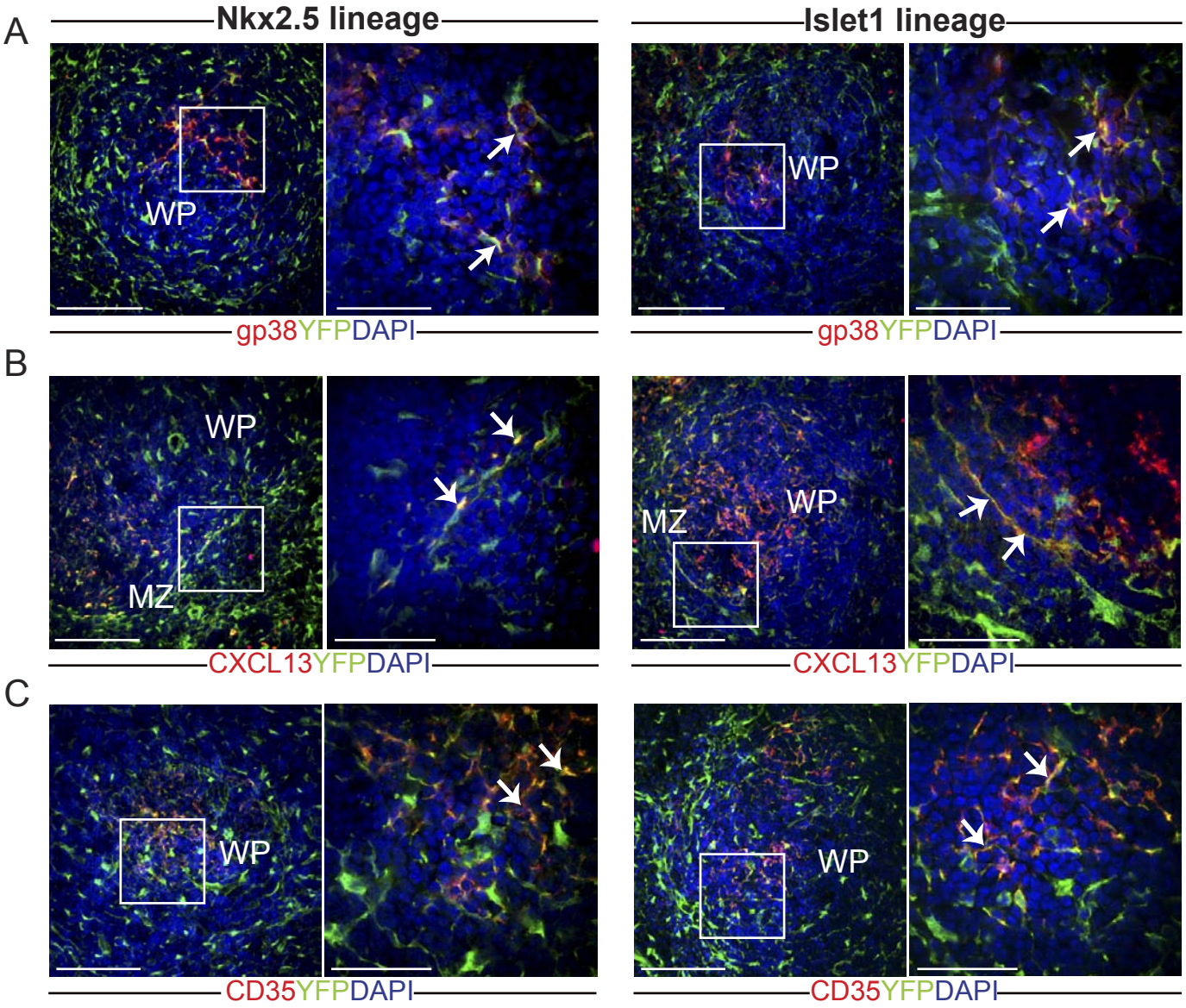
A
Nkx2.5 lineage
Islet1 lineage
WP
WP
gp38YFPDAPI
gp38YFPDAPI
B
WP
MZ
MZ
WP
CXCL13YFPDAPI
CXCL13YFPDAPI
C
WP
WP
CD35YFPDAPI
CD35YFPDAPI

Figure 3

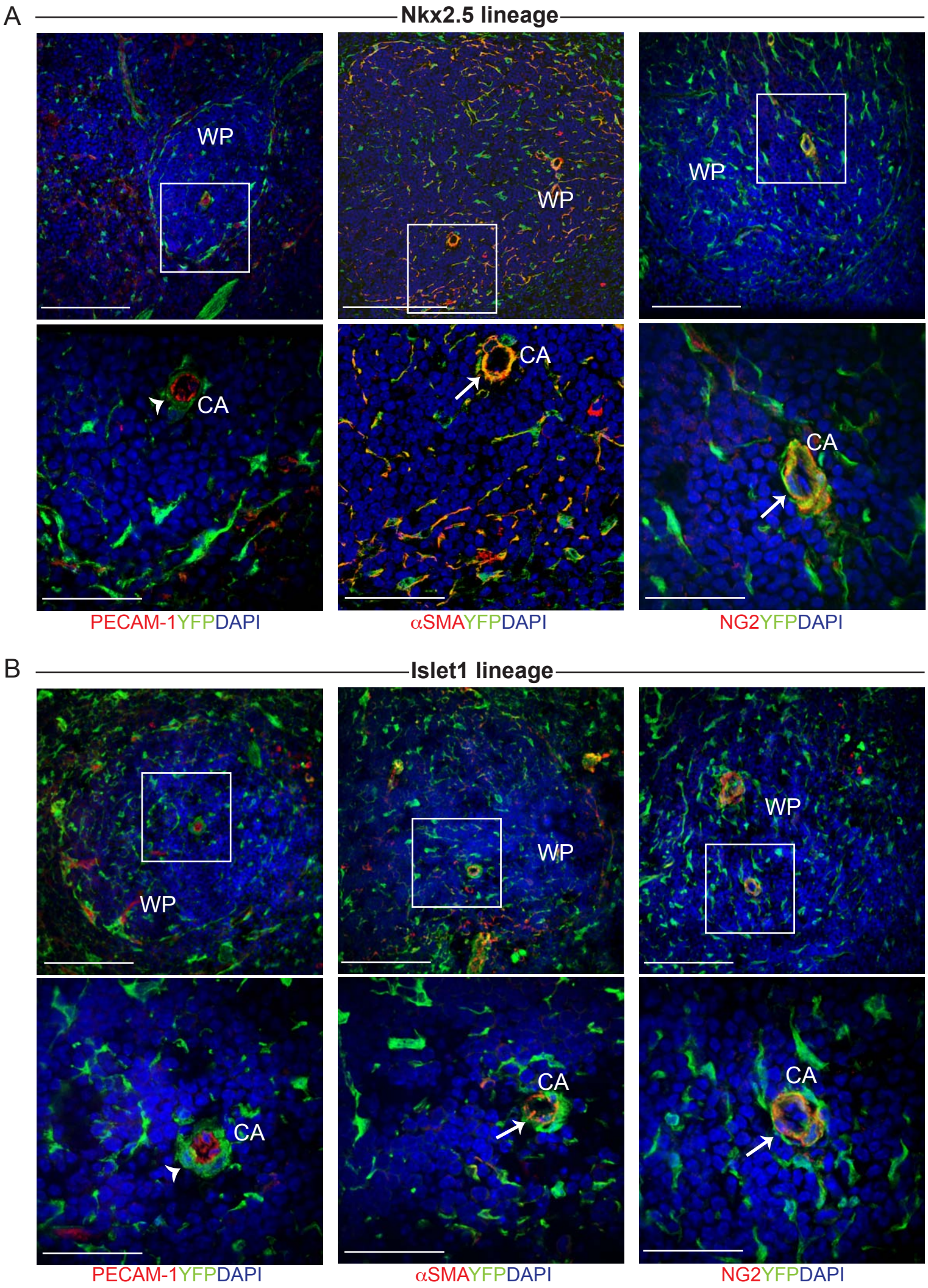
A
Nkx2.5 lineage
WP
WP
WP
CA
CA
CA
PECAM-1YFPDAPI
αSMAYFPDAPI
NG2YFPDAPI
B
Islet1 lineage
WP
WP
WP
CA
CA
CA
PECAM-1YFPDAPI
αSMAYFPDAPI
NG2YFPDAPI

Figure 4

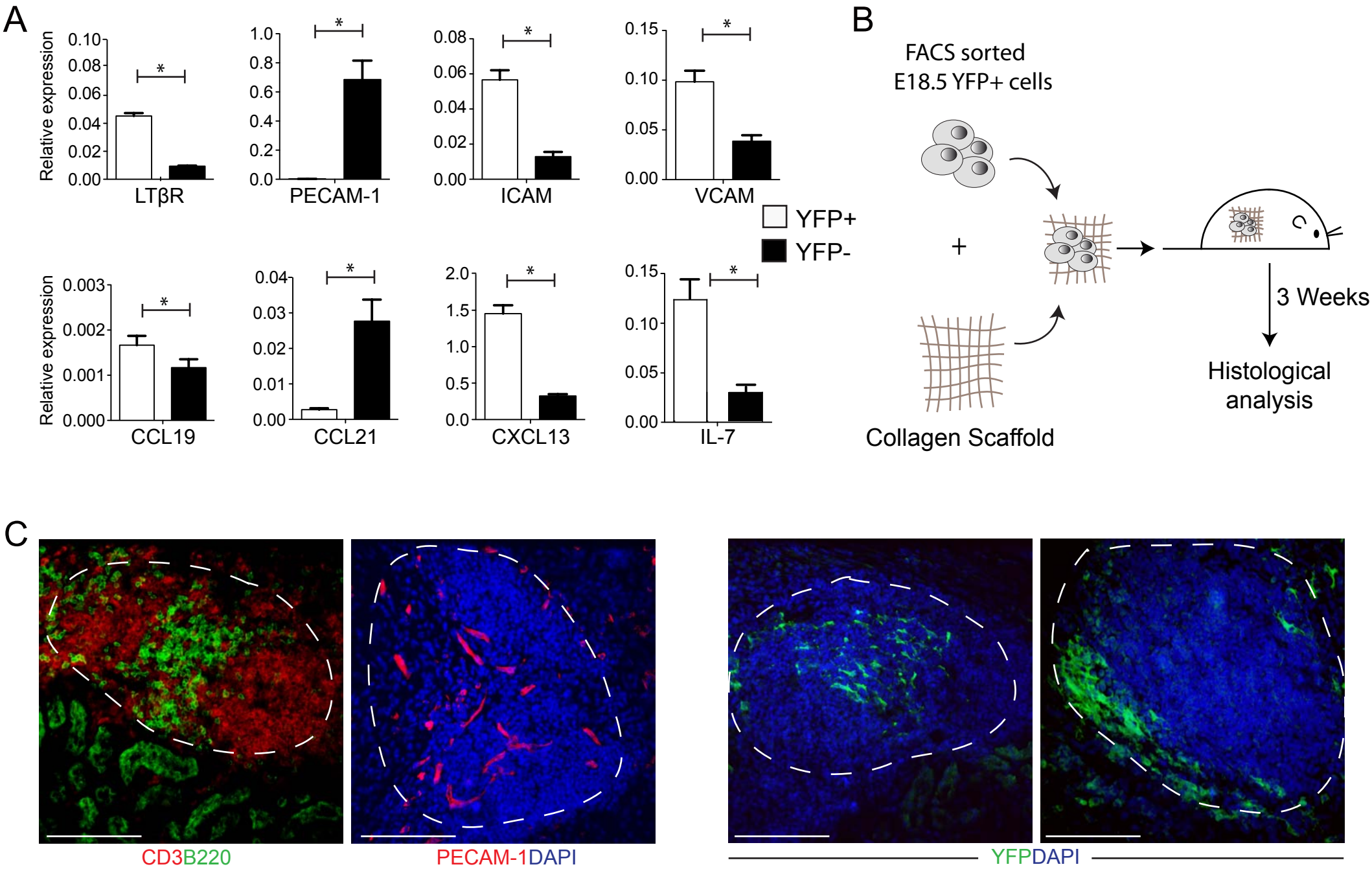
A
Relative expression
LTβR
PECAM-1
ICAM
VCAM
CCL19
CCL21
CXCL13
IL-7
YFP+
YFP-
B
FACS sorted
E18.5 YFP+ cells
+
Collagen Scaffold
3 Weeks
Histological
analysis
C
CD3B220
PECAM-1DAPI
YFPDAPI

Figure 5

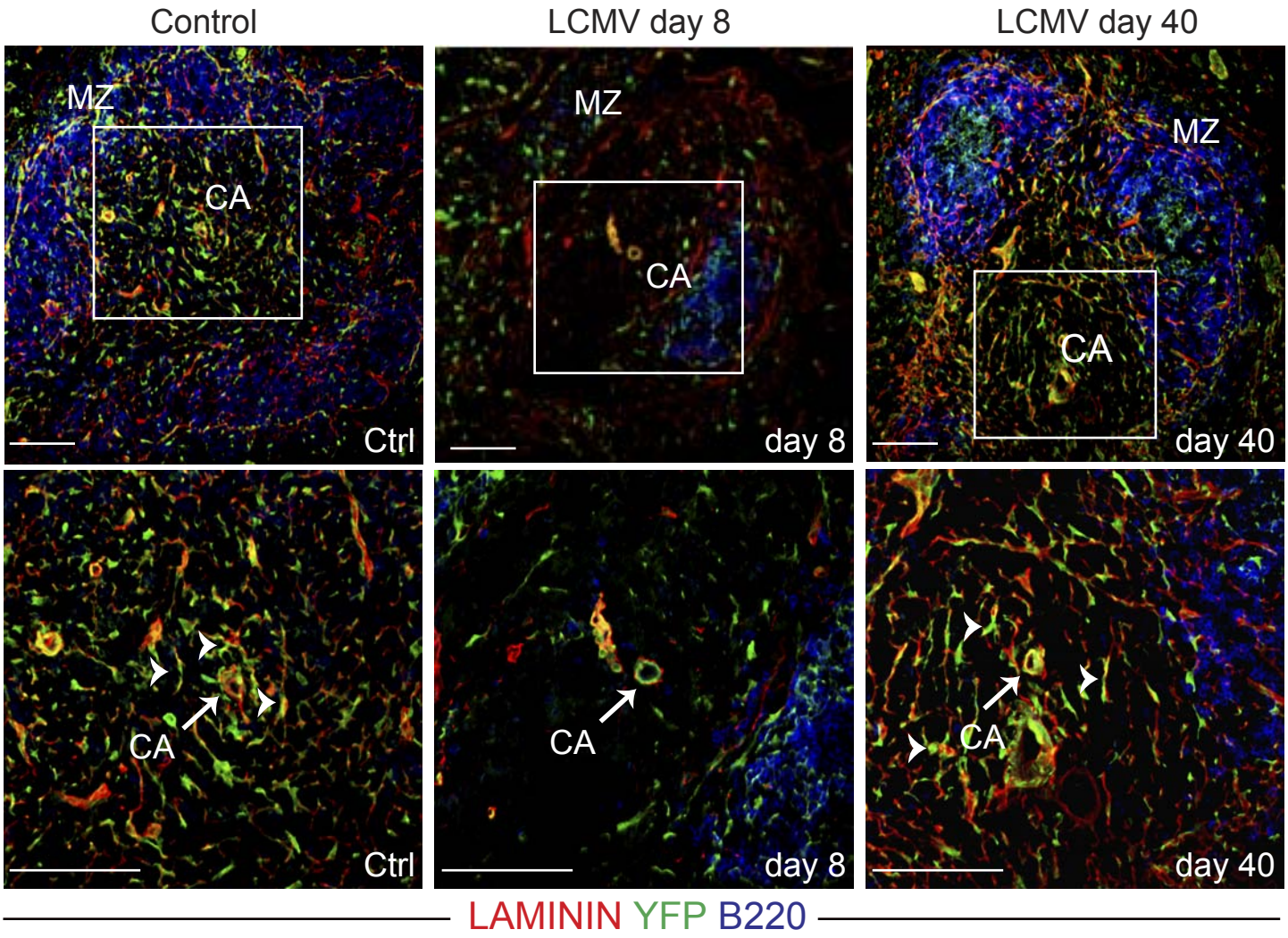
Control
LCMV day 8
LCMV day 40
MZ
CA
Ctrl
day 8
day 40
LAMININ YFP B220

Figure 6

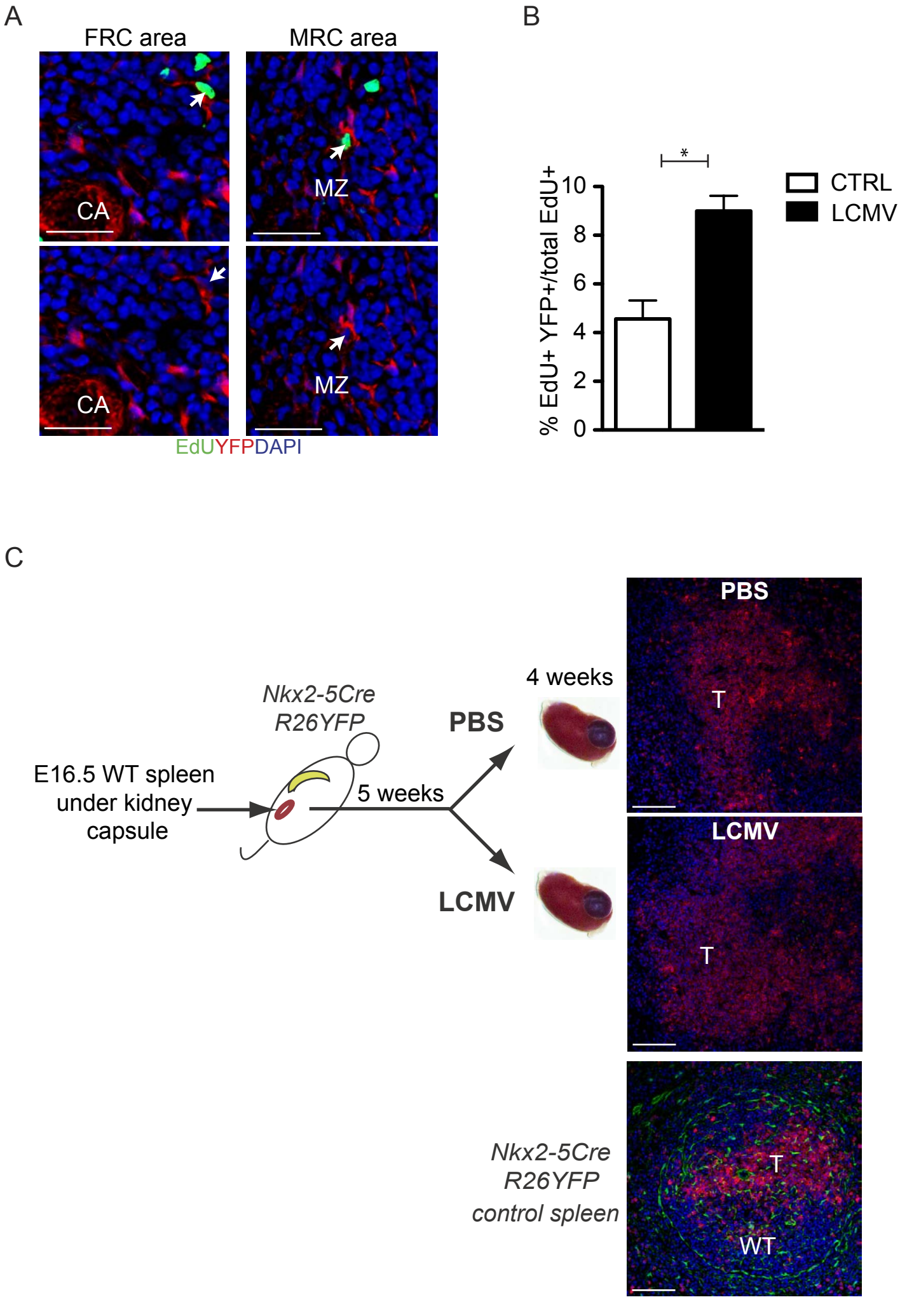
A
FRC area
MRC area
CA
MZ
CA
MZ
EdUYFPDAPI
B
*
% EdU+ YFP+/total EdU+
10
8
6
4
2
0
CTRL
LCMV
C
Nkx2-5Cre
R26YFP
E16.5 WT spleen
under kidney
capsule
5 weeks
PBS
LCMV
4 weeks
PBS
T
LCMV
T
Nkx2-5Cre
R26YFP
control spleen
T
WT
CD3YFPDAPI

Figure 7

A

Contribution of Nkx2-5 traced cells to adult spleen

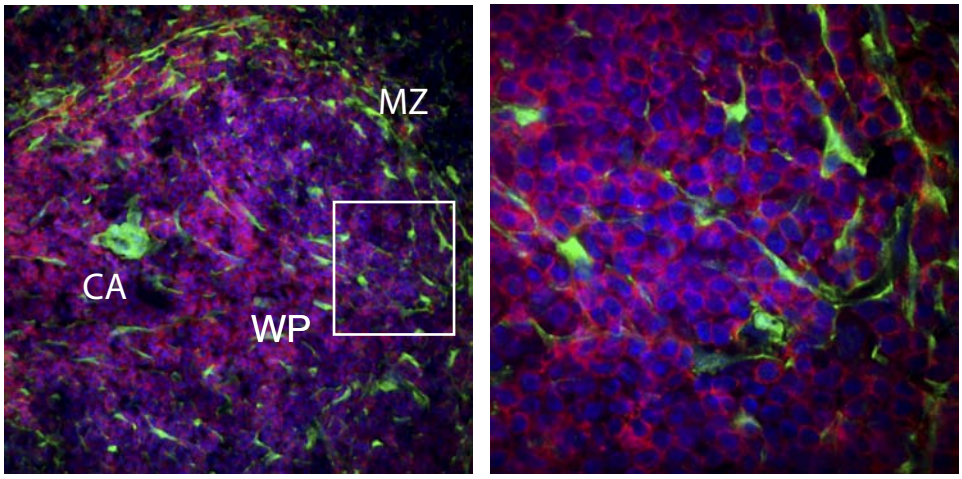

CD45YFPDAPI

B

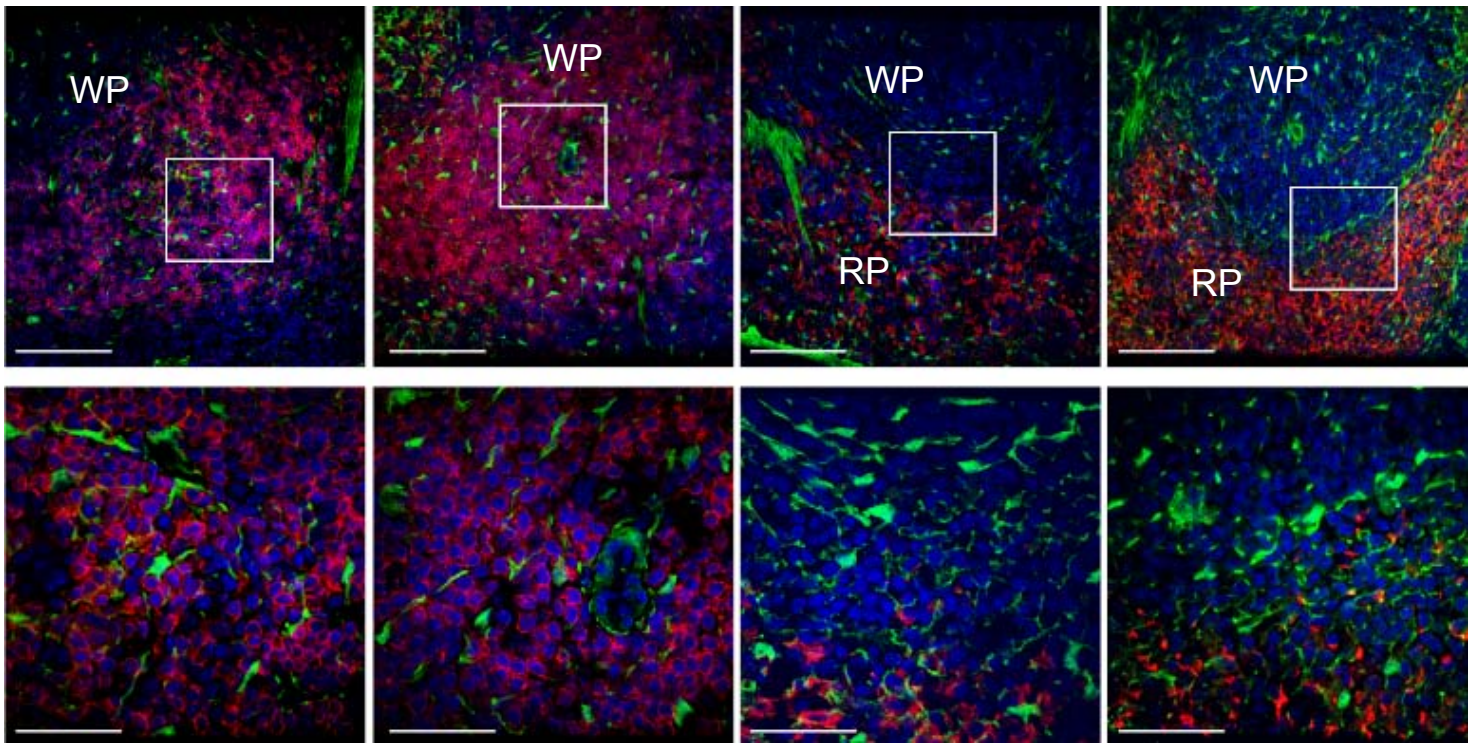

B220YFPDAPI CD3YFPDAPI F4/80YFPDAPI Ter119YFPDAPI

Suppl. Figure 1

A

Contribution of Islet1 traced cells to adult spleen

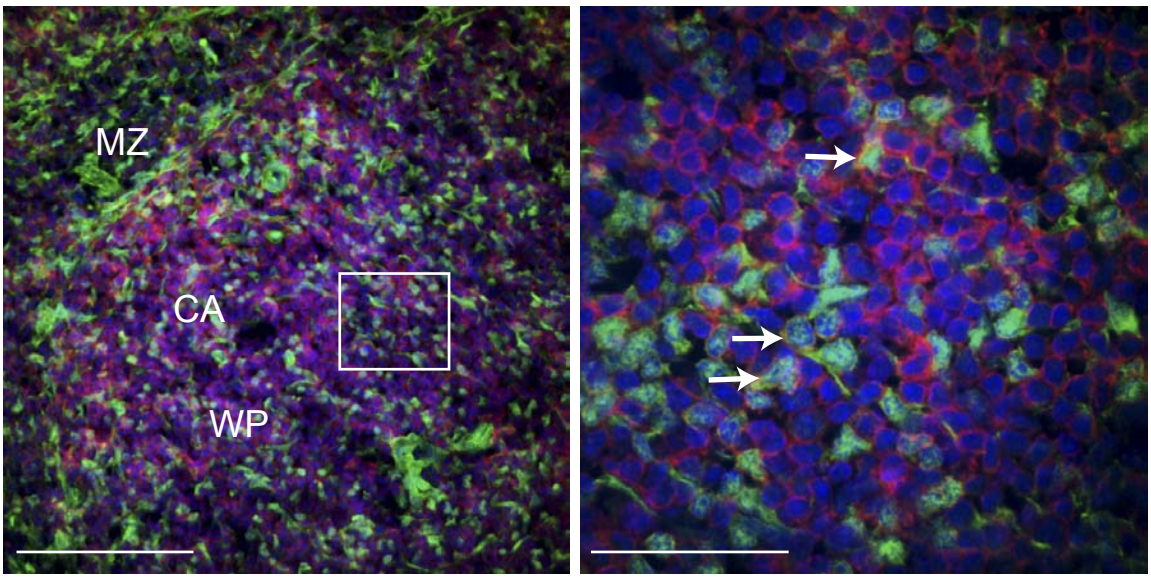

CD45YFPDAPI

B

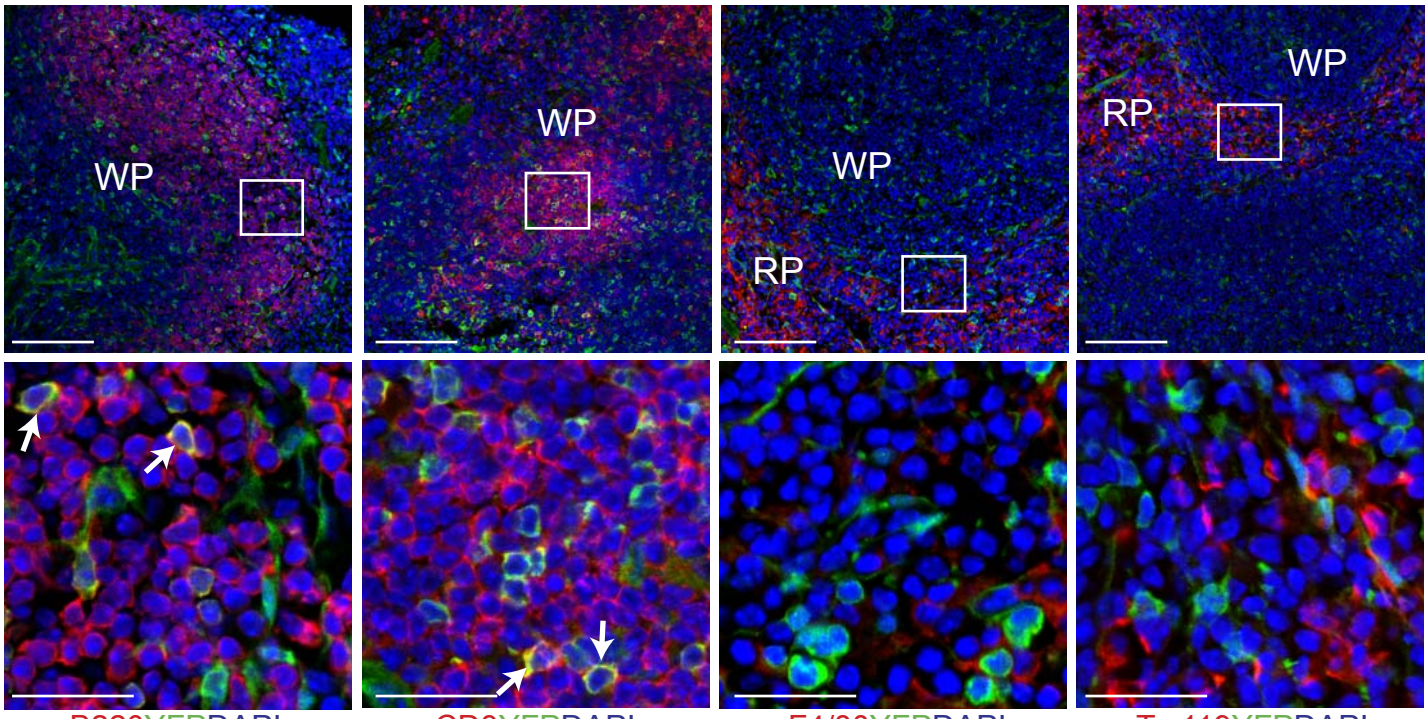

B220YFPDAPI CD3YFPDAPI F4/80YFPDAPI Ter119YFPDAPI

C

Islet1 expression in adult spleen

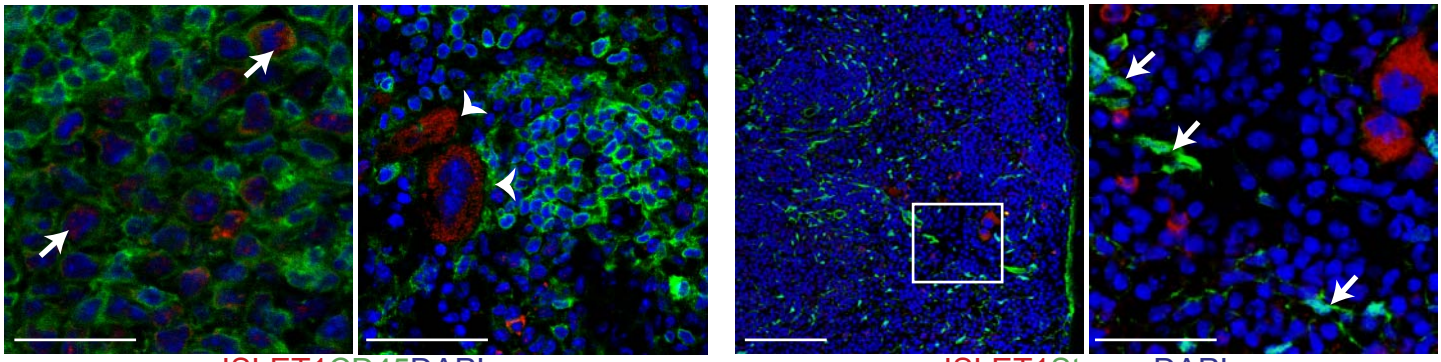

ISLET1CD45DAPI ISLET1StromaDAPI

Suppl. Figure 2

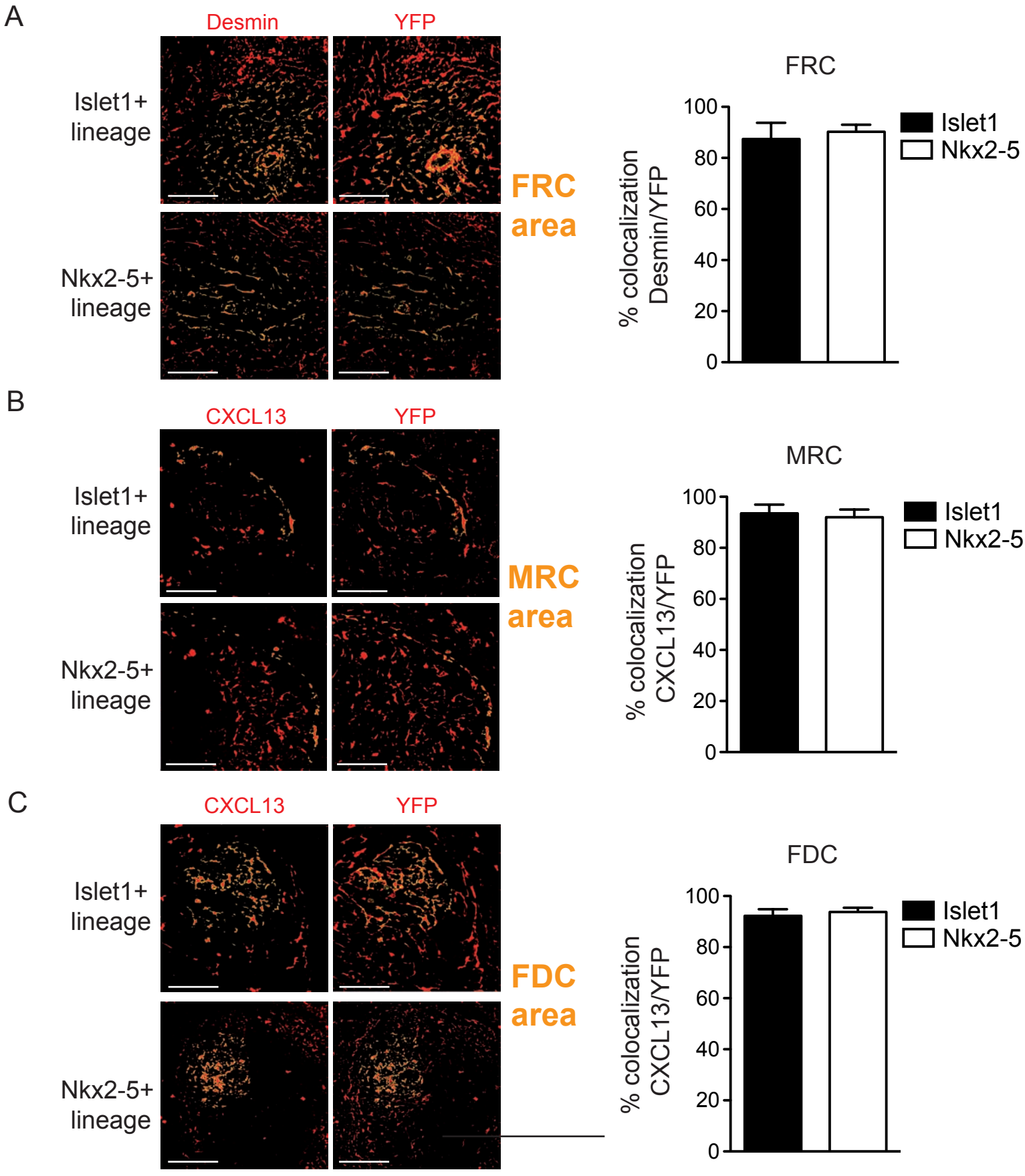

Suppl. Figure 3

T-cell area

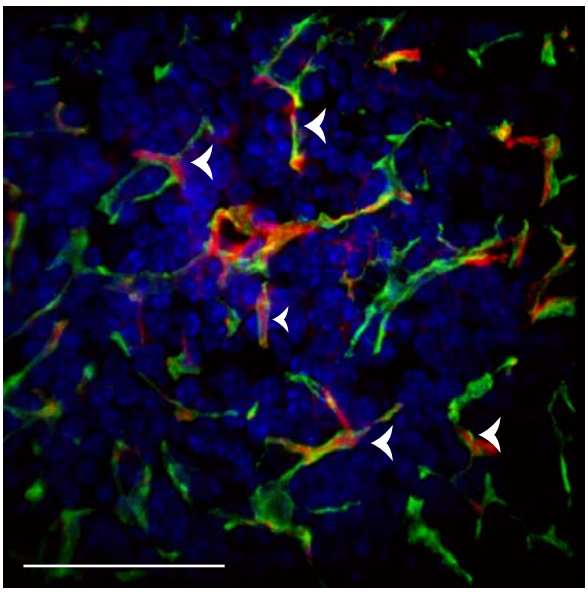

DEXTRANYFPDAPI

Suppl. Figure 4

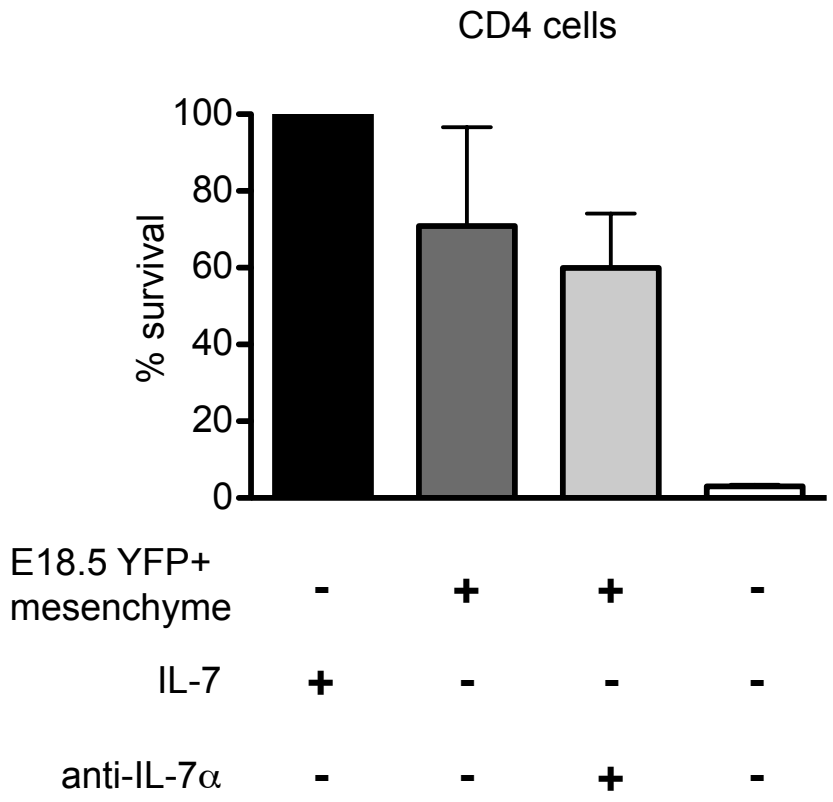

Suppl. Figure 5

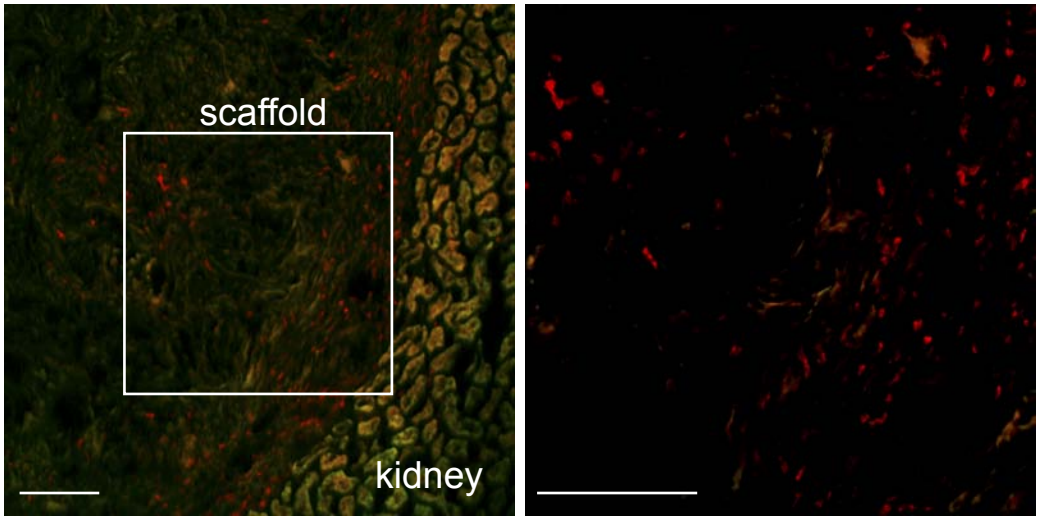

Suppl. Figure 6

A

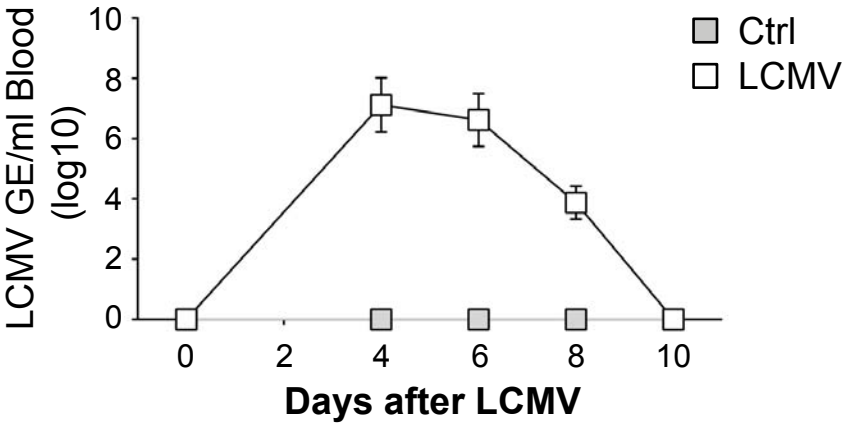

B

T-area

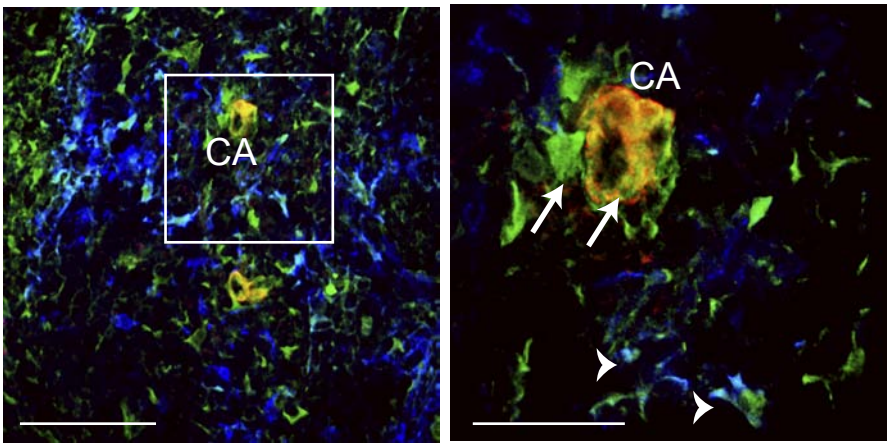

NG2YFPVL4

B-area

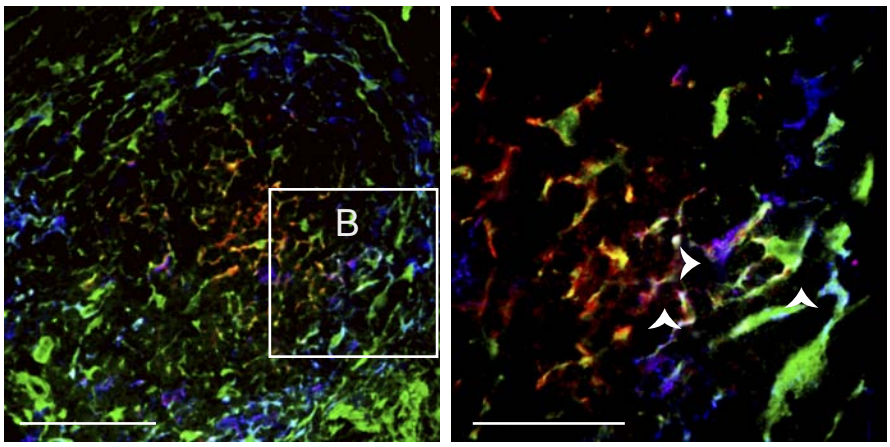

CD35YFPVL4

Marginal Zone

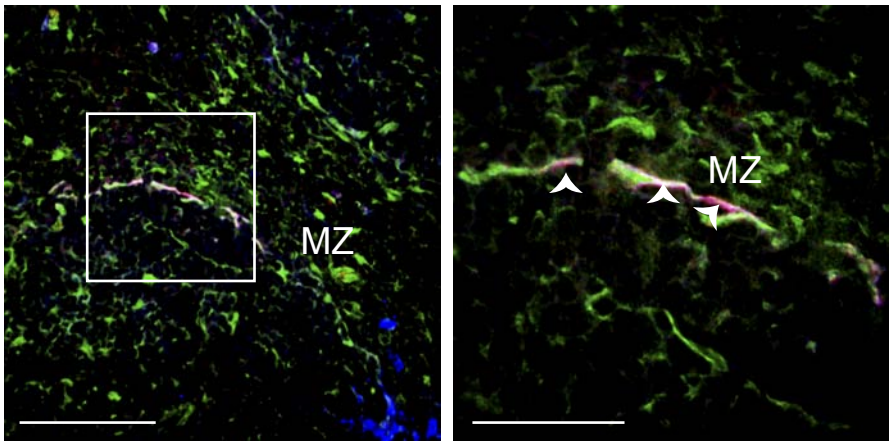

MAdCAM-1YFPVL4

Suppl. Figure 7

A

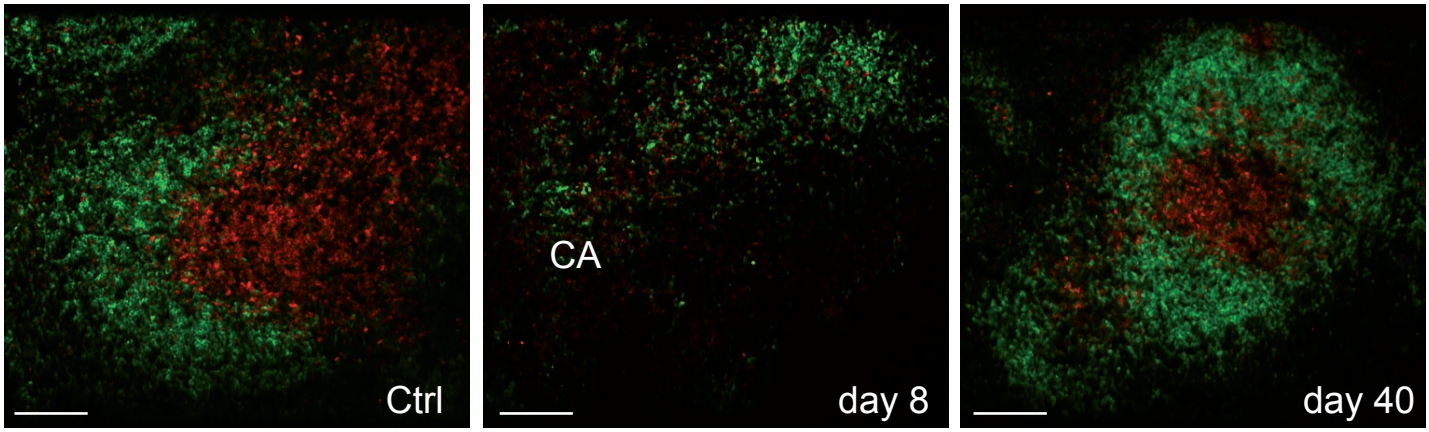

CD3B220

B

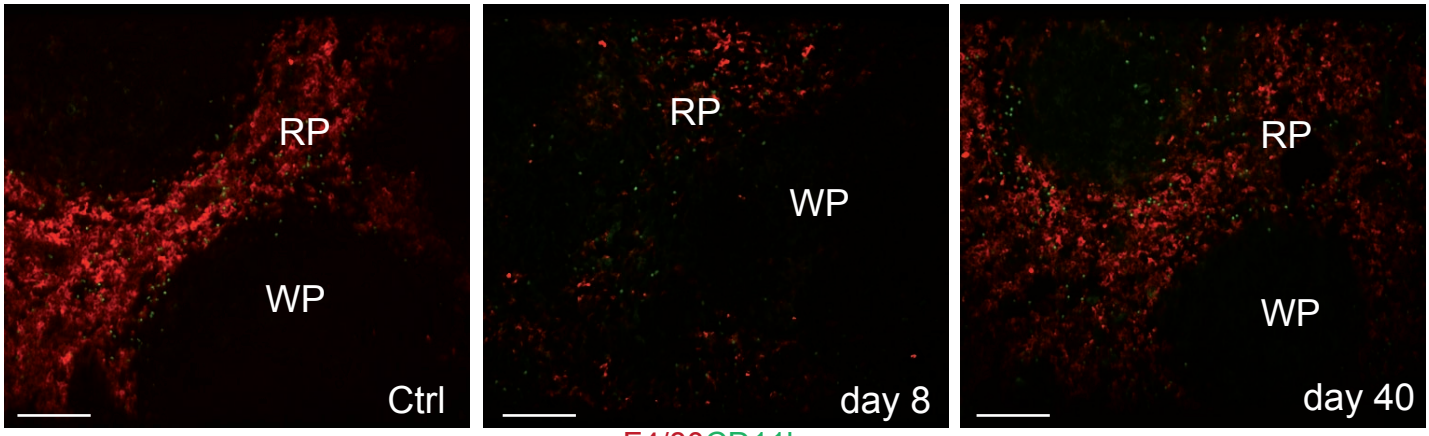

F4/80CD11b

Suppl. Figure 8